



HAL
open science

MEIOSIS INITIATES IN THE FETAL OVARY OF MICE LACKING ALL RETINOIC ACID RECEPTOR ISOTYPES

Nadège Vernet, Manuel Mark, Diana Condrea, Betty Féret, Muriel Klopfenstein, Violaine Alunni, Marius Teletin, Norbert B Ghyselinck

► **To cite this version:**

Nadège Vernet, Manuel Mark, Diana Condrea, Betty Féret, Muriel Klopfenstein, et al.. MEIOSIS INITIATES IN THE FETAL OVARY OF MICE LACKING ALL RETINOIC ACID RECEPTOR ISOTYPES. 2019. hal-02324110

HAL Id: hal-02324110

<https://hal.science/hal-02324110>

Preprint submitted on 21 Oct 2019

HAL is a multi-disciplinary open access archive for the deposit and dissemination of scientific research documents, whether they are published or not. The documents may come from teaching and research institutions in France or abroad, or from public or private research centers.

L'archive ouverte pluridisciplinaire **HAL**, est destinée au dépôt et à la diffusion de documents scientifiques de niveau recherche, publiés ou non, émanant des établissements d'enseignement et de recherche français ou étrangers, des laboratoires publics ou privés.

1 **MEIOSIS INITIATES IN THE FETAL OVARY OF MICE LACKING ALL RETINOIC**
2 **ACID RECEPTOR ISOTYPES**

3 Nadège VERNET¹, Manuel MARK^{1,2}, Diana CONDREA¹, Betty FÉRET¹, Muriel
4 KLOPFENSTEIN¹, Violaine ALUNNI³, Marius TELETIN^{1,2}, and Norbert B.
5 GHYSELINCK^{1*}

- 6 1. Institut de Génétique et de Biologie Moléculaire et Cellulaire (IGBMC),
7 Département de Génétique Fonctionnelle et Cancer, Centre National de la
8 Recherche Scientifique (CNRS UMR7104), Institut National de la Santé et de la
9 Recherche Médicale (INSERM U1258), Université de Strasbourg (UNISTRA),
10 1 rue Laurent Fries, BP-10142, F-67404 Illkirch Cedex, France
11 2. Service de Biologie de la Reproduction, Hôpitaux Universitaires de Strasbourg
12 (HUS), France
13 3. GenomEast platform, France Génomique consortium, IGBMC, 1 rue Laurent Fries,
14 F-67404 Illkirch Cedex, France

15 * Author for correspondence: norbert@igbmc.fr

16 Tel: +33 388 655 674; Fax: +33 388 653 201

17 **Abstract**

18 Gametes are generated through a specialized cell differentiation process,
19 meiosis which, in most mammals, is initiated in ovaries during fetal life. It is widely
20 admitted that all-*trans* retinoic acid (ATRA) is the molecular signal triggering meiosis
21 initiation in mouse female germ cells, but a genetic approach in which ATRA synthesis
22 is impaired disputes this proposal. In the present study, we investigated the
23 contribution of endogenous ATRA to meiosis by analyzing fetuses lacking all RARs
24 ubiquitously, obtained through a tamoxifen-inducible cre recombinase-mediated gene
25 targeting approach. Efficient ablation of RAR-coding genes was assessed by the
26 multiple congenital abnormalities displayed by the mutant fetuses. Unexpectedly, their
27 germ cells robustly expressed STRA8, REC8, SYCP1 and SYCP3, showing that RAR
28 are actually dispensable up to the zygotene stage of meiotic prophase I. Thus our study
29 goes against the current model according to which meiosis is triggered by endogenous
30 ATRA in the developing ovary and revives the identification of the meiosis-preventing
31 substance synthesized by CYP26B1 in the fetal testis.

32 **Introduction**

33 Mammalian meiosis is a germ-cell specific division process that generates
34 haploid gametes from their diploid precursors, oogonia in the female and
35 spermatogonia in the male. In the mouse, female germ cells enter into meiosis before
36 birth, around embryonic day 13.5 (E13.5)¹. During the same embryonic period, male
37 germ cells stop proliferating, and enter the G0/G1 phase of the cell cycle thus
38 becoming mitotically quiescent. Male germ cells resume proliferation at birth, and then
39 enter into meiosis starting from post-natal day 8².

40 In order to account for the sexual dimorphism in the timing of gem cell
41 differentiation, it was hypothesized, notably from transplantation experiments of germ
42 cells³, that the decision to enter meiosis is controlled by a meiosis-inducing substance
43 (MIS) or/and by a meiosis-preventing substance (MPS) produced by somatic cells⁴.
44 Subsequently, it was proposed that all-trans retinoic acid (ATRA) and its degrading
45 enzyme CYP26B1 played key roles in controlling the timing of meiosis initiation in
46 female and male gonads, respectively^{5,6}. The concept that ATRA is the MIS was
47 however challenged by a genetic study demonstrating that meiosis initiation occurs
48 despite the lack of two major ATRA-synthesizing enzymes⁷. The recent finding that a
49 third enzyme, expressed in fetal ovaries and capable of ATRA synthesis, is also
50 involved in meiosis revived the model according to which meiosis entry is triggered by
51 endogenous ATRA in the ovary⁸

52 ATRA is the active metabolite of retinol (vitamin A). Inside cells, conversion of
53 retinol to ATRA depends upon retinaldehyde dehydrogenases (ALDH1A1, ALDH1A2
54 and ALDH1A3 isotypes)⁹. Then, ATRA activity is mediated by the nuclear retinoic acid
55 receptors (RARA, RARB and RARG isotypes), which are ligand-dependent
56 transcriptional regulators. They usually function in the form of heterodimers with

57 retinoid receptors (RXRs) to control expression of ATRA-target genes, in which they
58 are bound to specific DNA sites called retinoic acid response elements (RARE)¹⁰. In
59 addition, RAR are capable of non-genomic activation events at the cell membrane¹¹,
60 similarly to steroid nuclear receptors¹².

61 As all ATRA-dependent events rely in some way on RAR, we decided to tackle
62 the potential contribution of endogenous ATRA to meiosis in female germ cells by
63 generating and analyzing mice lacking all RAR-isotypes. Against the currently admitted
64 model^{13,14}, our study reveals that RARs (and therefore endogenous ATRA) are in fact
65 fully dispensable for meiotic initiation in the mouse fetal ovary.

66 **Results**

67 **Expression of RARs in the fetal ovary**

68 The expression of *Rars* in the fetal gonads is poorly documented¹⁵⁻¹⁷. To
69 determine which RAR isotypes are actually present in the ovary, we performed
70 immunohistochemistry (IHC). At E11.5, RARA was detected in a large number of
71 tissues, including the somatic cells of the ovary but not germ cells (**Fig. 1A,C-E**). No
72 information was obtained for RARB since reliable antibodies for RARB are not
73 available¹⁸. RARG was readily detected in cartilages, but not in the ovary (**Fig. 1B-B'**).
74 Then we performed RT-qPCR on single ovarian cells at E13.5 (n=25) and E14.5 (n=40),
75 to which the germ cell identity was assigned based on the expression of *Dazl*, *Ddx4*
76 and *Kit*. *Rara* and *Rarg* mRNAs were detected in a majority of germ cells at E13.5 and
77 E14.5 (**Fig. 1F,G**). No information was obtained for *Rarb* mRNA since the mice we
78 used were on a *Rarb*-null genetic background (see Methods). It is therefore evident
79 that at least two RAR mRNAs are present in female germ cells, but at some stage their
80 level of expression is below the threshold of detection by IHC.

81 **Efficient ablation of all RARs in the developing gonad from E11.5 onwards**

82 Given the expression pattern of RARs, we reasoned that full impairment of ATRA
83 signaling in the whole fetal ovary would require the ablation of all three RAR-coding
84 genes. This was not possible by associating *Rara*, *Rarb* and *Rarg* knockout alleles in
85 a single fetus, because *Rara*^{-/-};*Rarg*^{-/-};*Rarb*^{+/-} embryos do not develop beyond E8.5,
86 precluding analysis of their ovaries¹⁹. To do so, we performed cre-directed genetic
87 ablation of *Rara* and *Rarg* using a ubiquitously expressed cre/ERT² activated by TAM,
88 prior to meiotic initiation, but later than E8.5, in the context of a *Rarb*-null background
89 (see Methods). We first chose to administer TAM at E10.5, shortly after the start of

90 gonad formation, but three days before meiosis initiation. Ablation of RARA and RARG
91 was assessed by IHC at E11.5, i.e., 24 hours after TAM-induction of cre/ERT².
92 Immunostaining for RARG was nearly abolished in mutant embryos in all RARG-
93 expressing tissues. Only a few cells reacted with the antibody (**Suppl. Fig. 1**). At E14.5,
94 the number of cells remaining positive for RARG in mutants was even smaller, while
95 no cell expressed RARA (**Suppl. Fig. 2**). Thus efficient ablation of RARA and RARG
96 was widespread at E11.5 and complete at E14.5.

97 The pattern of gene excision by cre/ERT² was assessed using the *mT/mG*
98 reporter transgene in control and mutant fetuses (see Methods). Expression of mGFP
99 was detected in all germ cells of the mutants at E11.5, and in almost all of them at
100 E14.5 (**Suppl. Fig. 3**). This indicated that cre/ERT²-directed excision of the reporter
101 occurred in almost all germ cells, as early as 24 hours after TAM treatment. In
102 agreement with this finding, *Rara* and *Rarg* mRNAs were not detected in any germ cell
103 isolated from mutant ovaries at E13.5 or E14.5, and analyzed by RT-qPCR (**Fig. 1G**).
104 Altogether, these data showed that efficient excision of all RARs occurred in all germ
105 cells.

106 **Ablation of all RARs does not impair meiosis initiation**

107 To investigate the impact of RAR ablation on meiotic initiation, the expression of
108 canonical markers of meiosis was assessed by IHC throughout the anteroposterior
109 axis of the ovary. At E14.5, numerous germ cells in both control and mutant fetuses
110 expressed the synaptonemal protein SYCP3²⁰ and the cohesin REC8²¹ (**Fig. 2A**). The
111 mean number of germ cells, and the percentages of SYCP3-positive or REC8-positive
112 germ cells were similar in control and mutant fetuses (**Fig. 2B,C**). This indicated that
113 meiosis initiated in germ cells of the mutant fetuses.

114 To rule out the possibility that the cells which initiated meiosis experienced an
115 inefficient ablation of the RAR-coding genes, we took advantage of the presence of
116 *mT/mG* reporter in the fetuses. The vast majority of the SYCP3- or REC8-positive germ
117 cells of the mutant ovary were mGFP-positive (**Fig. 3A-F**), indicating excision in almost
118 all of the meiotic cells. Surprisingly, mGFP was never detected in somatic cells of the
119 ovary nor in the mesonephros, making questionable whether cre/ERT² was efficient or
120 whether the reporter was expressed in these cells. To assess RAR ablation in somatic
121 cells and exclude the possibility that cre-mediated excision was mosaic, we performed
122 genomic PCR analysis, using DNA extracted from whole ovaries of E13.5 control and
123 mutant fetuses. Excised (L-), but not conditional (L2), alleles of *Rara* and *Rarg* were
124 detected in genomic DNA isolated from mutant ovaries. In contrast, conditional (L2),
125 but not excised (L-), alleles were always detected in control ovaries (**Fig. 3G,H**).
126 Altogether, these data show that efficient excision of all RARs occurs in all of their
127 tissues, including somatic and germ cells in the ovaries.

128 To further investigate expression of the meiotic program at the cellular level in the
129 absence of RARs, we used RT-qPCR on single cells isolated from ovaries at E13.5
130 (25 control and 43 mutant germ cells) and E14.5 (40 control and 47 mutant germ cells).
131 Consistent with IHC analyses, the proportion of germ cells expressing *Sycp3* and *Rec8*,
132 as well as their individual levels of expression, were similar in control and mutant
133 ovaries (**Fig. 3I**). In addition, the cellular expression of 12 other meiosis-specific genes
134 including some of the ATRA-dependent class 1 to 3 genes²² (*Dmc1*, *Mei1*, *Meiob*,
135 *Prdm9*, *Smc1b*, *Spo11*, *Stag3*, *Syce1*, *Syce2*, *Sycp1*, *Sycp2*, *Ugt8a*) was similar,
136 whether RAR were present or absent (**Suppl. Figs. 4-6**). This confirmed the
137 commitment of mutant germ cells toward meiosis, despite their lack of RARs.

138 Importantly, the meiotic gatekeeper STRA8²³ was also expressed in germ cells
139 of mutant ovaries, notably in those which underwent cre/ERT²-mediated recombination
140 (**Fig. 3C,F**), albeit their number was about half-less that observed in control ovaries
141 (**Fig. 2C**). Accordingly, *Stras8* mRNA was present in only 30% of the germ cells from
142 mutant ovaries at E13.5, versus 92% in control ovaries. In addition, its expression level
143 was slightly decreased, when compared to the control situation (**Fig. 3I**). This
144 difference was smoothed out at E14.5 in mutant germ cells where the expression level
145 of *Stras8* almost reached that measured in control germ cells at E13.5 (**Fig. 3I**). These
146 observation suggested that *Stras8* expression might be delayed in the absence of RARs.

147 **Ablation of RARs at an earlier developmental stage dramatically impacts** 148 **embryonic development but not meiosis initiation**

149 When treated by TAM at 10.5, the mutant fetuses displayed, at E14.5, some of
150 the eye defects typically observed in *Rarb*^{-/-};*Rarg*^{-/-} knockout fetuses (**Suppl. Fig. 7**).
151 However, overall these mutant fetus were much less malformed than expected from
152 previous works²⁴. For instance, the cardiac defects described in *Rara*^{-/-};*Rarg*^{-/-}
153 knockout fetuses²⁵ were not observed. To test for the possibility that this discrepancy
154 could be due to the timing of RARs ablation, we treated pregnant females with TAM at
155 E9.5, and analyzed the phenotypes induced in fetuses at E14.5. The mutants
156 generated in this way displayed most of the congenital malformations that are
157 hallmarks of the loss of RARs²⁴ (**Fig. 4**). We conclude therefore that deletion of RARs
158 with TAM at E9.5 recapitulates the pathological phenotypes observed in the compound
159 knockouts of RARs (i.e., in *Rara*^{-/-};*Rarb*^{-/-}, *Rara*^{-/-};*Rarg*^{-/-} and *Rarb*^{-/-};*Rarg*^{-/-} fetuses).

160 Given the role assigned to ATRA in sex determination²⁶ and primordial germ cells
161 proliferation^{27,28}, one might have expected that deleting RARs at E9.5 would affect the

162 gonads more dramatically than at E10.5. Yet, ovaries formed in mutants and contained
163 normal amounts of germ cells, out of which many of them were meiotic, as indicated
164 by their expression of SYCP3 at E14.5 (**Suppl. Fig. 8**).

165 To test for the possibility of a delay in meiosis entry in the absence of RAR (see
166 above), we analyzed at E15.5 control and mutant ovaries of fetuses treated by TAM at
167 E9.5. Virtually all germ cells had entered meiosis in the mutant ovaries, as attested by
168 the detection of SYCP3 in almost all germ cells (**Fig. 5A,B**). Moreover, a majority of
169 the germ cells showed thread-like segments of synaptonemal complexes positive for
170 only SYCP3 or SYCP1 and SYCP3, indicating that they were at the late leptotene to
171 zygotene stages (**Fig. 5C,D**). Both REC8 and STRA8 were detected at E15.5 in a few
172 germ cells from control and mutant ovaries (**Fig. 5E-H**), as expected from previous
173 studies^{29,30}. Altogether, our results indicate that RARs are indispensable neither to
174 enter meiosis, nor to express STRA8 in germ cells. Importantly, no increase of
175 apoptosis was evidenced in the mutant ovaries, excluding thereby the possibility that
176 some of the RAR-deficient germ cells experienced cell-death. We conclude that in
177 females, RARs are not required for gonad differentiation nor for meiosis, up to the
178 zygotene stage.

179 Discussion

180 It is widely believed that ATRA synthesized by the mesonephros is an essential
181 paracrine factor diffusing into the ovary to trigger the differentiation of oogonia to
182 oocytes, which progress into meiosis^{13,31-36}. Nonetheless, germ cells can initiate
183 meiosis in the absence of ALDH1A2, the ATRA-synthesizing enzyme detected in the
184 mesonephros⁷. This seemingly contradictory data has been the source of heated and
185 passionate debates^{14,37} but the discovery that the weak ATRA-synthesizing enzyme
186 ALDH1A1 is capable of generating some ATRA in the developing mouse ovary^{8,38}
187 tailored an explanation for the finding that ovarian germ cells remain able to enter
188 meiosis in *Aldh1a2*^{-/-} knockout fetuses^{8,35}. We designed the present genetic study, in
189 which ATRA-receptors are deleted, to address by another mean the question as to
190 whether or not ATRA is required to meiosis initiation in the mouse female germ cells.

191 Our results clearly show that meiotic cells expressing STRA8, REC8 and SYCP3
192 are present in ovaries lacking RARs. Both the number of STRA8-positive cells and the
193 level of *Stras8* expression are lower in mutant than in control ovaries at E13.5. However,
194 this difference diminishes at E14.5, and at E15.5 the proportion of oocytes that are at
195 the late leptotene and zygotene stages is similar in mutant and control ovaries. It is
196 therefore reasonable to propose that RARs participate to the timed expression of *Stras8*
197 in the fetal ovary but, are actually not indispensable. Actually, other transcription factors
198 such as MSX1, MSX2³⁹ and DMRT1⁴⁰, other signaling pathways such as BMPs^{39,41}
199 and Activin A⁴², as well as the epigenetic status of chromatin^{43,44} appear more
200 important than ATRA for proper *Stras8* expression in the fetal ovary.

201 More intriguingly, single cell RT-qPCR analyses at E13.5 reveal that some control
202 and most RAR-null oocytes express meiotic genes such as *Dmc1*, *Smc1b*, *Spo11*,
203 *Stag3*, *Syce1*, *Syce2*, before expressing *Stras8*. Nonetheless, meiosis progresses up

204 to the zygotene stage at E15.5, despite the delay in *Stra8* expression. This finding
205 suggests that *Stra8* expression is not be the primary event triggering meiosis in oocytes,
206 which is unexpected given its assigned central role in this process²³. Accordingly,
207 *Stra8*-deficient ovarian germ cells can grow and differentiate into oocyte-like cells,
208 without premeiotic chromosomal replication, synapsis and recombination⁴⁵. Analysis
209 of RAR-deficient oocytes beyond zygotene would certainly be informative, but is
210 unfortunately not possible because RAR-null mutant fetuses die at birth from multiple
211 congenital abnormalities²⁴.

212 The finding that RARs are crucial for neither *Stra8* expression nor meiosis
213 initiation implies that ATRA is not the molecule triggering meiosis, provided it does not
214 act through a RAR-independent mechanism. Several reports describe binding of ATRA
215 to nuclear receptors other than RARs. First, peroxisome proliferator activated receptor
216 delta (PPARD) is activated by ATRA when the latter is delivered bound to FABP5. The
217 interaction of ATRA with PPARD has a Kd of 15–50 nM⁴⁶, more than two order of
218 magnitude weaker than that of RAR, which is in the 0.1–0.2 nM range^{47,48}. This
219 concentration of ATRA is much higher than that observed in the fetal mouse ovary⁷ or
220 required for *Stra8* expression³⁶. In addition, *Fabp5* is not expressed in the mouse fetal
221 ovary¹⁶, and *Ppard*-null females are fertile, indicating normal meiosis^{49,50}. Second, the
222 chicken ovalbumin upstream promoter transcription factor (NR2F2) and the testicular
223 receptor 4 (NR2C2) can be activated by ATRA, but at non-physiological concentrations
224 of 10-30 μ M^{51,52}. Third, ATRA binds to the retinoic acid receptor-related orphan
225 receptor beta (RORB) with a Kd of 0.3 μ M, but *Rorb*-null females are fertile⁵³. Aside
226 from nuclear receptors, cellular retinoic acid binding protein 1 (CRABP1) is also able
227 to mediate some non-genomic activity of ATRA at a concentration of 100 nM⁵⁴.
228 However, CRABP1-null mice are fertile, and their ovaries appears fully normal⁵⁵⁻⁵⁷.

229 Since all the mechanisms identified to date through which ATRA could act
230 independently of RARs can be excluded, ATRA is not the meiosis inducing substance.
231 In agreement with this view, the report by Chassot et al. (accompanying manuscript)
232 shows that simultaneous ablation of *Aldh1a1*, *Aldh1a2* and *Aldh1a3* in either the
233 somatic cells or in the whole ovary of mice do not impair *Stra8* expression and meiosis
234 initiation. These findings are in keeping with the recent observation that initiation of
235 meiosis and expression of *Stra8* by spermatocytes occurs without ATRA⁵⁸.

236 Our results apparently contradict previous observations^{13,31-36}, but several
237 explanations can be proposed to reconcile the discrepancies. First, experiments
238 performed using BMS-204493^{6,29,41} and AGN193109^{5,8,26,38} to impair ATRA signaling
239 in fetal ovaries or testes must be interpreted with caution. Actually these ligands are
240 not RAR antagonists, as they are usually referred to as, but pan-RAR inverse agonists,
241 which are capable of repressing RAR basal activity by favoring and stabilizing
242 recruitment of corepressors, even in the absence of an endogenous agonistic ligand
243 such as ATRA⁵⁹⁻⁶². As RAR binding sites are present in the *Stra8* promoter on which
244 RARs are actually bound *in vivo*^{7,63,64}, adding a pan-RAR inverse agonist predictably
245 induces recruitment of NCOR1 and NCOR2 corepressors at the locus, promotes
246 chromatin compaction⁶⁵ and thereby *Stra8* extinction, irrespective of the presence of
247 ATRA in the ovary. The same holds true for the *Rec8* gene, which also contains a
248 RARE^{63,66}. The fact that expression of these two genes is artificially shut down upon
249 exposure to a pan-RAR inverse agonist does not mean that their expression is normally
250 controlled by endogenous ATRA. If one assumes that *Rec8* and *Stra8* are actually not
251 regulated by endogenous ATRA, it is perfectly logical to find them expressed in germ
252 cells lacking RARs (present study). For the same reason, the fact that AGN193109
253 abrogates the ectopic expression of *Stra8* in *Cyp26b1*-null mouse testes is not a proof

254 that expression of *Stra8* depends on ATRA signaling. Therefore it cannot be used as
255 an argument to quash the theory proposed by Kumar et al. in 2011 that a molecule
256 distinct from ATRA is involved in the initiation of meiosis⁸. Second, it has been
257 recurrently emphasized that alterations generated by exogenously administered ATRA
258 do not necessarily reflect physiological processes^{24,67-69}. In the case of the gonads, the
259 simple fact that RAR-binding sites are present in *Stra8* and *Rec8* genes can explain
260 their forced expression and initiation of meiosis by supra-physiological concentrations
261 of ATRA added to fetal rat ovaries⁷⁰ and to mouse testes cultured *in vitro*^{5,6}.

262 Involvement of ATRA in meiosis is commonly interpreted according to the
263 prevailing idea according which both a MIS, ATRA, and a MPS, the ATRA-degrading
264 enzyme CYP26B1, are required to account for the sex-specific timing of meiotic
265 initiation^{13,14}. Since the present work disqualifies ATRA as an MIS, the “MPS-only”
266 hypothesis⁷¹ would reconcile the discrepancies present in the literature: germ cells are
267 programmed to initiate meiosis unless prevented from doing so by an MPS produced
268 in the testis⁷². According to this scenario, inducing mitotic quiescence instead of
269 meiosis in male germ cells during fetal life requires a yet unknown substance, the MPS,
270 which is undoubtedly produced by CYP26B1^{7,73}. Efforts should now be put to identify
271 this substance.

272 **Methods**

273 **Mice and treatments**

274 Mice were on a mixed C57BL/6 (50%)/129/SvPass (50%) genetic background. They
275 were housed in a licensed animal facility (agreement #C6721837). All experiments
276 were approved by the local ethical committee (Com'Eth, accreditations APAFIS#5638-
277 2016061019045714 and APAFIS#5639-201606101910981), and were supervised by
278 N.B.G., M.M. and N.V., who are qualified in compliance with the European Community
279 guidelines for laboratory animal care and use (2010/63/UE). To inactivate *Rar* coding
280 genes, mice bearing *loxP*-flanked (L2) alleles of *Rara*⁷⁴ and *Rarg*⁷⁵ and null (L-) alleles
281 of *Rarb*^{76,77} were crossed with mice bearing the ubiquitously expressed, tamoxifen-
282 inducible, *cre/ERT*² recombinase-coding *Tg(Ubc-cre/ERT*² transgene⁷⁸. Females
283 homozygous for L2 alleles of *Rara* and *Rarg* and for L- alleles of *Rarb* (i.e.,
284 *Rara*^{L2/L2};*Rarg*^{L2/L2};*Rarb*^{L-/L-}) were mated with males bearing one copy of the *Tg(Ubc-*
285 *cre/ERT*²), and homozygous for L2 alleles of *Rara* and *Rarg* and for L- alleles of *Rarb*
286 (i.e., *Tg(Ubc-cre/ERT*²);*Rara*^{L2/L2};*Rarg*^{L2/L2};*Rarb*^{L-/L-}). Noon of the day of a vaginal plug
287 was taken as 0.5 day embryonic development (E0.5). To activate the *cre/ERT*²
288 recombinase in embryos, one tamoxifen (TAM) treatment (130 mg/kg body weight)
289 was administered to the pregnant females by oral gavage at E9.5 or at E10.5. TAM
290 (T5648, Sigma-Aldrich) was dissolved in ethanol at a concentration of 100 mg/mL and
291 further diluted in sunflower oil to a concentration of 10 mg/ml. This resulted in embryos
292 or fetuses null for *Rarb* in which *Rara* and *Rarg* were ablated upon TAM induction when
293 they were bearing *Tg(Ubc-cre/ERT*²) (referred to as mutants), as well as their control
294 littermates when the embryos or fetuses were free of *Tg(Ubc-cre/ERT*²) (referred to as
295 controls). Importantly, embryos, fetuses and females null for *Rarb* display normal
296 ovaries and are totally fertile^{76,77}. To assess for *cre/ERT*²-directed excision, we

297 introduced the *Gt(ROSA26)^{ACTB-tdTomato-EGFP}* reporter transgene (referred to as *mT/mG*),
298 which directs expression of a membrane-targeted green fluorescent protein (mGFP) in
299 cells that have experienced cre-mediated deletion⁷⁹, in the *Tg(Ubc-*
300 *cre/ERT²); Rara^{L2/L2}; Rarg^{L2/L2}; Rarb^{L-/L-}* genetic background. Embryos and fetuses were
301 collected by caesarean section and the yolk sacs, tail biopsies or female gonads were
302 taken for DNA extraction. Genotypes were determined as described^{74-76,78,79}.

303 **External morphology, histology and immunohistochemistry**

304 Following collection, E11.5 embryos to E15.5 fetuses were fixed overnight in cold 4%
305 (w/v) paraformaldehyde (PFA) in phosphate buffered saline (PBS). After removal of
306 the fixative, embryos and fetuses were rapidly rinsed in PBS and placed in 70% (v/v)
307 ethanol for long-term storage and external morphology evaluation. They were next
308 embedded in paraffin. Consecutive, frontal, 5 µm-thick sections were made throughout
309 the entire specimens. For histology, sections were stained with hematoxylin and eosin
310 (H&E). For immunohistochemistry (IHC) antigen were retrieved for 1 hour at 95°C
311 either in 10 mM sodium citrate buffer at pH 6.0 or, only in the case of IHC for detection
312 of REC8 and SYCP1, in Tris-EDTA at pH 9.0 [10 mM Tris Base, 1 mM EDTA, 0.05%
313 (v/v) Tween 20]. Sections were rinsed in PBS, then incubated with appropriate dilutions
314 of the primary antibodies or a mixture of them (i.e., anti-DDX4 and anti-SYCP3; anti-
315 SYCP1 and anti-SYCP3) in PBS containing 0.1% (v/v) Tween 20 (PBST) for 16 h at
316 4°C in a humidified chamber. After rinsing in PBST (3 times for 3 min each), detection
317 of the bound primary antibodies was achieved for 45 min at 20°C in a humidified
318 chamber using Cy3-conjugated donkey anti-rabbit, Alexa Fluor 488-conjugated
319 donkey anti-mouse or goat anti-chicken antibodies, depending on the origin of the
320 primary antibody depending on the origin of the primary antibody (**Suppl. Table 1**).

321 Nuclei were counterstained with 4',6-diamidino-2-phenyl-indole (DAPI) diluted at
322 10 µg/ml in the mounting medium (Vectashield; Vector).

323 **Characterization and counts of the meiotic germ cells**

324 Germ cell counts were performed on pairs of fetuses consisting of one mutant and one
325 of its control littermates, and each experiment was repeated on at least 3 different
326 fetuses per genotype, age and stage of TAM treatment. The total number of germ cells
327 in ovaries of control and mutant E14.5 fetuses was quantified using immunostaining
328 for DDX4. Meiotic germ cells were quantified using immunostaining for SYCP3, REC8
329 and STRA8. A double-immunostaining for SYCP1 and SYCP3 was performed to detect
330 germ cells at the zygotene stage. Data were expressed as percentages related to the
331 number of DDX4-positive cells. Statistical analysis was done by a two-tail Student *t*-
332 test, assuming unequal variances after arcsine transformation of the percentages of
333 germ cells expressing the meiotic markers.

334 **Single cell RT-qPCR and data processing**

335 Gonads from E13.5 and E14.5 control and mutant fetuses were dissected out in PBS
336 and sexed by their appearance under the microscope. Ovaries were separated from
337 mesonephros using the cutting edge of a 25G needle. Dissociated cells were obtained
338 by incubating the gonads for 15 minutes in PBS containing 0.5 µM EDTA⁸⁰. To allow
339 cell pricking, gonads were then transferred in PBS containing 4 mg/ml BSA. Cells were
340 released by puncture of the gonad with 25G needles. This technique generally resulted
341 in a suspension of germ cells, which are recognized as large, refringent, cells, with low
342 somatic cell contamination⁸¹. Cells (n=88 at E13.5 and n=132 at E14.5), were collected
343 individually using pulled Pasteur pipets, and transferred as isolated, single, cells into
344 micro-tubes containing 5 µl of cold 1X SuperScript IV VILO Master Mix for two-step
345 RT-qPCR containing 6 units RNasin (Promega) and 0.5% (v/v) NP40. The micro-tubes

346 were then stored at -80°C for later processing. Two-step, single-cell, gene expression
347 analysis was achieved on the BioMark HD system (Fluidigm) using SsoFast EvaGreen
348 Supermix with low ROX (Bio-Rad Laboratories) according to manufacturer's
349 instructions. The set of primers used for qPCR are listed (**Suppl. Table 2**). Cts were
350 recovered and analyzed by the Fluidigm Real-Time PCR Analysis software, using the
351 linear (derivative) baseline correction method and the auto (global) Ct threshold
352 method. Limit of detection (LOD) was set to a Ct of 28. The quality threshold was set
353 to 0.65. Cts for qPCR reactions that failed the quality threshold (melting curves with
354 deviating T_m temperatures) were converted to 28. The Ct values were then exported
355 to Excel and converted to expression levels using the equation
356 $\text{Log Ex} = \text{Ct}[\text{LOD}] - \text{Ct}[\text{Assay}]$. The expressions of *Actb* and *Tbp* housekeeping genes
357 were measured to determine which sample actually contained a cell. Cells that fail to
358 amplify systematically all the tested genes or to express germ cell markers (*Dazl*, *Ddx4*
359 and *Kit*) were excluded from further analysis. The percentages of cells excluded was
360 23% at E13.5 and 34% at E14.5. This can be explained by the greater difficulty to
361 isolate and collect germ cells at E14.5, compared to E13.5. The final analysis was done
362 using n=68 individual cells at E13.5 (n=25 controls, n=43 mutants) and n=87 individual
363 cells at E14.5 (n=40 controls, n=47 mutants). Results were not normalized relative to
364 housekeeping genes, as their expression did not differ between control and mutant
365 cells. Percentages of cells expressing a gene of interest are represented as histograms,
366 and expression levels are represented as violin and box plot using R Studio software.

367 **References**

- 368 1 Borum, K. Oogenesis in the mouse. A study of the meiotic prophase. *Exp. Cell*
369 *Res.* **24**, 495-507 (1961).
- 370 2 Drumond, A. L., Meistrich, M. L. & Chiarini-Garcia, H. Spermatogonial
371 morphology and kinetics during testis development in mice: a high-resolution light
372 microscopy approach. *Reproduction* **142**, 145-155 (2011).
- 373 3 McLaren, A. Germ cells and germ cell sex. *Philos. Trans. R. Soc. Lond. B Biol.*
374 *Sci.* **350**, 229-233 (1995).
- 375 4 Byskov, A. G. & Saxen, L. Induction of meiosis in fetal mouse testis in vitro. *Dev.*
376 *Biol.* **52**, 193-200 (1976).
- 377 5 Bowles, J. et al. Retinoid signaling determines germ cell fate in mice. *Science*
378 **312**, 596-600 (2006).
- 379 6 Koubova, J. et al. Retinoic acid regulates sex-specific timing of meiotic initiation
380 in mice. *Proc. Natl. Acad. Sci. USA* **103**, 2474-2479 (2006).
- 381 7 Kumar, S. et al. Sex-specific timing of meiotic initiation is regulated by Cyp26b1
382 independent of retinoic acid signalling. *Nat. Commun.* **2**, 151 (2011).
- 383 8 Bowles, J. et al. ALDH1A1 provides a source of meiosis-inducing retinoic acid in
384 mouse fetal ovaries. *Nat. Commun.* **7**, 10845 (2016).
- 385 9 Duester, G. Involvement of alcohol dehydrogenase, short-chain
386 dehydrogenase/reductase, aldehyde dehydrogenase, and cytochrome P450 in
387 the control of retinoid signaling by activation of retinoic acid synthesis.
388 *Biochemistry* **35**, 12221-12227 (1996).
- 389 10 Chambon, P. The nuclear receptor superfamily: a personal retrospect on the first
390 two decades. *Mol. Endocrinol.* **19**, 1418-1428 (2005).
- 391 11 Al Tanoury, Z., Piskunov, A. & Rochette-Egly, C. Vitamin A and retinoid signaling:
392 genomic and nongenomic effects. *J. Lipid Res.* **54**, 1761-1775 (2013).
- 393 12 Losel, R. & Wehling, M. Nongenomic actions of steroid hormones. *Nat. Rev. Mol.*
394 *Cell Biol.* **4**, 46-56 (2003).
- 395 13 Bowles, J. & Koopman, P. Retinoic acid, meiosis and germ cell fate in mammals.
396 *Development* **134**, 3401-3411 (2007).
- 397 14 Griswold, M. D., Hogarth, C. A., Bowles, J. & Koopman, P. Initiating meiosis: the
398 case for retinoic acid. *Biol. Reprod.* **86**, 35 (2012).
- 399 15 Dolle, P., Ruberte, E., Leroy, P., Morriss-Kay, G. & Chambon, P. Retinoic acid
400 receptors and cellular retinoid binding proteins. I. A systematic study of their
401 differential pattern of transcription during mouse organogenesis. *Development*
402 **110**, 1133-1151 (1990).

- 403 16 Jameson, S. A. et al. Temporal transcriptional profiling of somatic and germ cells
404 reveals biased lineage priming of sexual fate in the fetal mouse gonad. *PLoS*
405 *Genet.* **8**, e1002575 (2012).
- 406 17 Ruberte, E. et al. Specific spatial and temporal distribution of retinoic acid
407 receptor gamma transcripts during mouse embryogenesis. *Development* **108**,
408 213-222 (1990).
- 409 18 Vernet, N. et al. Retinoic acid metabolism and signaling pathways in the adult
410 and developing mouse testis. *Endocrinology* **147**, 96-110 (2006).
- 411 19 Wendling, O., Ghyselinck, N. B., Chambon, P. & Mark, M. Roles of retinoic acid
412 receptors in early embryonic morphogenesis and hindbrain patterning.
413 *Development* **128**, 2031-2038 (2001).
- 414 20 Yuan, L. et al. The synaptonemal complex protein SCP3 can form multistranded,
415 cross-striated fibers in vivo. *J. Cell Biol.* **142**, 331-339 (1998).
- 416 21 Eijpe, M., Offenberg, H., Jessberger, R., Revenkova, E. & Heyting, C. Meiotic
417 cohesin REC8 marks the axial elements of rat synaptonemal complexes before
418 cohesins SMC1beta and SMC3. *J. Cell Biol.* **160**, 657-670 (2003).
- 419 22 Soh, Y. Q. et al. A Gene Regulatory Program for Meiotic Prophase in the Fetal
420 Ovary. *PLoS Genet.* **11**, e1005531 (2015).
- 421 23 Baltus, A. E. et al. In germ cells of mouse embryonic ovaries, the decision to enter
422 meiosis precedes premeiotic DNA replication. *Nat. Genet.* **38**, 1430-1434 (2006).
- 423 24 Mark, M., Ghyselinck, N. B. & Chambon, P. Function of retinoid nuclear receptors:
424 lessons from genetic and pharmacological dissections of the retinoic acid
425 signaling pathway during mouse embryogenesis. *Annu. Rev. Pharmacol. Toxicol.*
426 **46**, 451-480 (2006).
- 427 25 Lohnes, D. et al. Function of the retinoic acid receptors (RARs) during
428 development (I). Craniofacial and skeletal abnormalities in RAR double mutants.
429 *Development* **120**, 2723-2748 (1994).
- 430 26 Bowles, J. et al. Retinoic Acid Antagonizes Testis Development in Mice. *Cell Rep.*
431 **24**, 1330-1341 (2018).
- 432 27 Koshimizu, U., Watanabe, M. & Nakatsuji, N. Retinoic acid is a potent growth
433 activator of mouse primordial germ cells in vitro. *Dev. Biol.* **168**, 683-685 (1995).
- 434 28 Tedesco, M., Desimio, M. G., Klinger, F. G., De Felici, M. & Farini, D. Minimal
435 concentrations of retinoic acid induce stimulation by retinoic acid 8 and promote
436 entry into meiosis in isolated pregonadal and gonadal mouse primordial germ
437 cells. *Biol. Reprod.* **88**, 145 (2013).
- 438 29 Koubova, J. et al. Retinoic acid activates two pathways required for meiosis in
439 mice. *PLoS Genet.* **10**, e1004541 (2014).

- 440 30 Menke, D. B., Koubova, J. & Page, D. C. Sexual differentiation of germ cells in
441 XX mouse gonads occurs in an anterior-to-posterior wave. *Dev. Biol.* **262**, 303-
442 312 (2003).
- 443 31 Agrimson, K. S. & Hogarth, C. A. Germ Cell Commitment to Oogenic Versus
444 Spermatogenic Pathway: The Role of Retinoic Acid. *Results Probl. Cell Differ.* **58**,
445 135-166 (2016).
- 446 32 Bowles, J. & Koopman, P. Sex determination in mammalian germ cells: extrinsic
447 versus intrinsic factors. *Reproduction* **139**, 943-958 (2010).
- 448 33 Bowles, J. & Koopman, P. Precious cargo: regulation of sex-specific germ cell
449 development in mice. *Sex Dev.* **7**, 46-60 (2013).
- 450 34 Feng, C. W., Bowles, J. & Koopman, P. Control of mammalian germ cell entry
451 into meiosis. *Mol. Cell. Endocrinol.* **382**, 488-497 (2014).
- 452 35 Spiller, C. & Bowles, J. Sexually dimorphic germ cell identity in mammals. *Curr.*
453 *Top. Dev. Biol.* **134**, 253-288 (2019).
- 454 36 Spiller, C. M., Bowles, J. & Koopman, P. Regulation of germ cell meiosis in the
455 fetal ovary. *Int. J. Dev. Biol.* **56**, 779-787 (2012).
- 456 37 Kumar, S., Cunningham, T. J. & Duyster, G. Resolving molecular events in the
457 regulation of meiosis in male and female germ cells. *Sci. Signal* **6**, pe25 (2013).
- 458 38 Mu, X. et al. Retinoic acid derived from the fetal ovary initiates meiosis in mouse
459 germ cells. *J. Cell Physiol.* **228**, 627-639 (2013).
- 460 39 Le Bouffant, R. et al. Msx1 and Msx2 promote meiosis initiation. *Development*
461 **138**, 5393-5402 (2011).
- 462 40 Krentz, A. D. et al. DMRT1 promotes oogenesis by transcriptional activation of
463 Stra8 in the mammalian fetal ovary. *Dev. Biol.* **356**, 63-70 (2011).
- 464 41 Miyauchi, H. et al. Bone morphogenetic protein and retinoic acid synergistically
465 specify female germ-cell fate in mice. *EMBO J.* **36**, 3100-3119 (2017).
- 466 42 Liang, G. J. et al. Activin A accelerates the progression of fetal oocytes
467 throughout meiosis and early oogenesis in the mouse. *Stem Cells Dev.* **24**, 2455-
468 2465 (2015).
- 469 43 Wang, N. & Tilly, J. L. Epigenetic status determines germ cell meiotic commitment
470 in embryonic and postnatal mammalian gonads. *Cell Cycle* **9**, 339-349 (2010).
- 471 44 Yokobayashi, S. et al. PRC1 coordinates timing of sexual differentiation of female
472 primordial germ cells. *Nature* **495**, 236-240 (2013).
- 473 45 Dokshin, G. A., Baltus, A. E., Eppig, J. J. & Page, D. C. Oocyte differentiation is
474 genetically dissociable from meiosis in mice. *Nat. Genet.* **45**, 877-883 (2013).

- 475 46 Tan, N. S. et al. Selective cooperation between fatty acid binding proteins and
476 peroxisome proliferator-activated receptors in regulating transcription. *Mol. Cell.*
477 *Biol.* **22**, 5114-5127 (2002).
- 478 47 Dong, D., Ruuska, S. E., Levinthal, D. J. & Noy, N. Distinct roles for cellular
479 retinoic acid-binding proteins I and II in regulating signaling by retinoic acid. *J.*
480 *Biol. Chem.* **274**, 23695-23698 (1999).
- 481 48 Sussman, F. & de Lera, A. R. Ligand recognition by RAR and RXR receptors:
482 binding and selectivity. *J. Med. Chem.* **48**, 6212-6219 (2005).
- 483 49 Barak, Y. et al. Effects of peroxisome proliferator-activated receptor delta on
484 placentation, adiposity, and colorectal cancer. *Proc. Natl. Acad. Sci. USA* **99**,
485 303-308 (2002).
- 486 50 Peters, J. M. et al. Growth, adipose, brain, and skin alterations resulting from
487 targeted disruption of the mouse peroxisome proliferator-activated receptor
488 beta(delta). *Mol. Cell. Biol.* **20**, 5119-5128 (2000).
- 489 51 Kruse, S. W. et al. Identification of COUP-TFII orphan nuclear receptor as a
490 retinoic acid-activated receptor. *PLoS Biol.* **6**, e227 (2008).
- 491 52 Zhou, X. E. et al. The orphan nuclear receptor TR4 is a vitamin A-activated
492 nuclear receptor. *J. Biol. Chem.* **286**, 2877-2885 (2011).
- 493 53 Andre, E. et al. Disruption of retinoid-related orphan receptor beta changes
494 circadian behavior, causes retinal degeneration and leads to vacillans phenotype
495 in mice. *EMBO J.* **17**, 3867-3877 (1998).
- 496 54 Persaud, S. D. et al. All trans-retinoic acid analogs promote cancer cell apoptosis
497 through non-genomic Crabp1 mediating ERK1/2 phosphorylation. *Sci. Rep.* **6**,
498 22396 (2016).
- 499 55 de Bruijn, D. R. et al. Normal development, growth and reproduction in cellular
500 retinoic acid binding protein-I (CRABPI) null mutant mice. *Differentiation* **58**, 141-
501 148 (1994).
- 502 56 Gorry, P. et al. The cellular retinoic acid binding protein I is dispensable. *Proc.*
503 *Natl. Acad. Sci. USA* **91**, 9032-9036 (1994).
- 504 57 Lampron, C. et al. Mice deficient in cellular retinoic acid binding protein II
505 (CRABPII) or in both CRABPI and CRABPII are essentially normal. *Development*
506 **121**, 539-548 (1995).
- 507 58 Teletin, M. et al. Two functionally redundant sources of retinoic acid secure
508 spermatogonia differentiation in the seminiferous epithelium. *Development* **146**,
509 pii: dev170225 (2019).
- 510 59 Germain, P. et al. Differential action on coregulator interaction defines inverse
511 retinoid agonists and neutral antagonists. *Chem. Biol.* **16**, 479-489 (2009).

- 512 60 Germain, P., Iyer, J., Zechel, C. & Gronemeyer, H. Co-regulator recruitment and
513 the mechanism of retinoic acid receptor synergy. *Nature* **415**, 187-192 (2002).
- 514 61 Klein, E. S. et al. Identification and functional separation of retinoic acid receptor
515 neutral antagonists and inverse agonists. *J. Biol. Chem.* **271**, 22692-22696
516 (1996).
- 517 62 Klein, E. S., Wang, J. W., Khalifa, B., Gavigan, S. A. & Chandraratna, R. A.
518 Recruitment of nuclear receptor corepressor and coactivator to the retinoic acid
519 receptor by retinoid ligands. Influence of DNA-heterodimer interactions. *J. Biol.*
520 *Chem.* **275**, 19401-19408 (2000).
- 521 63 Chatagnon, A. et al. RAR/RXR binding dynamics distinguish pluripotency from
522 differentiation associated cis-regulatory elements. *Nucleic Acids Res.* **43**, 4833-
523 4854 (2015).
- 524 64 Giuili, G. et al. Murine spermatogonial stem cells: targeted transgene expression
525 and purification in an active state. *EMBO Rep.* **3**, 753-759 (2002).
- 526 65 Rosenfeld, M. G., Lunnyak, V. V. & Glass, C. K. Sensors and signals: a
527 coactivator/corepressor/epigenetic code for integrating signal-dependent
528 programs of transcriptional response. *Genes Dev.* **20**, 1405-1428 (2006).
- 529 66 Mahony, S. et al. Ligand-dependent dynamics of retinoic acid receptor binding
530 during early neurogenesis. *Genome Biol.* **12**, R2 (2011).
- 531 67 Cunningham, T. J. & Duester, G. Mechanisms of retinoic acid signalling and its
532 roles in organ and limb development. *Nat. Rev. Mol. Cell Biol.* **16**, 110-123 (2015).
- 533 68 Ghyselinck, N. B. & Duester, G. Retinoic acid signaling pathways. *Development*
534 **146**, pii: dev167502 (2019).
- 535 69 Horton, C. & Maden, M. Endogenous distribution of retinoids during normal
536 development and teratogenesis in the mouse embryo. *Dev. Dyn.* **202**, 312-323
537 (1995).
- 538 70 Livera, G., Rouiller-Fabre, V., Valla, J. & Habert, R. Effects of retinoids on the
539 meiosis in the fetal rat ovary in culture. *Mol. Cell. Endocrinol.* **165**, 225-231 (2000).
- 540 71 Kocer, A., Reichmann, J., Best, D. & Adams, I. R. Germ cell sex determination in
541 mammals. *Mol. Hum. Reprod.* **15**, 205-213 (2009).
- 542 72 McLaren, A. & Southee, D. Entry of mouse embryonic germ cells into meiosis.
543 *Dev. Biol.* **187**, 107-113 (1997).
- 544 73 MacLean, G., Li, H., Metzger, D., Chambon, P. & Petkovich, M. Apoptotic
545 extinction of germ cells in testes of Cyp26b1 knockout mice. *Endocrinology* **148**,
546 4560-4567 (2007).
- 547 74 Chapellier, B. et al. A conditional floxed (loxP-flanked) allele for the retinoic acid
548 receptor alpha (RARalpha) gene. *Genesis* **32**, 87-90 (2002).

- 549 75 Chapellier, B. et al. A conditional floxed (loxP-flanked) allele for the retinoic acid
550 receptor gamma (RARgamma) gene. *Genesis* **32**, 95-98 (2002).
- 551 76 Chapellier, B. et al. A conditional floxed (loxP-flanked) allele for the retinoic acid
552 receptor beta (RARbeta) gene. *Genesis* **32**, 91-94 (2002).
- 553 77 Ghyselinck, N. B. et al. Role of the retinoic acid receptor beta (RARbeta) during
554 mouse development. *Int. J. Dev. Biol.* **41**, 425-447 (1997).
- 555 78 Ruzankina, Y. et al. Deletion of the developmentally essential gene ATR in adult
556 mice leads to age-related phenotypes and stem cell loss. *Cell Stem Cell* **1**, 113-
557 126 (2007).
- 558 79 Muzumdar, M. D., Tasic, B., Miyamichi, K., Li, L. & Luo, L. A global double-
559 fluorescent Cre reporter mouse. *Genesis* **45**, 593-605 (2007).
- 560 80 De Felici, M. & McLaren, A. Isolation of mouse primordial germ cells. *Exp. Cell*
561 *Res.* **142**, 476-482 (1982).
- 562 81 Adams, I. R. & McLaren, A. Sexually dimorphic development of mouse primordial
563 germ cells: switching from oogenesis to spermatogenesis. *Development* **129**,
564 1155-1164 (2002).

565 **Acknowledgments**

566 We thank Dr Amandine Chassot, Dr Marie-Christine Chaboissier and Dr Eric Pailhoux
567 for discussions, advices and critical reading of the manuscript. We also thank Dr
568 Christelle Thibault-Carpentier from the Genomeast platform for her input
569 (<http://genomeast.igbmc.fr/>). This work was supported by grants from CNRS, INSERM,
570 UNISTRA and Agence Nationale pour la Recherche (ANR; 10-BLAN-1239, 13-BSV6-
571 0003 and 13-BSV2-0017), as well as from EU (FP7-PEOPLE-IEF-2012-331687). Their
572 studies were also supported in part by the grant ANR-10-LABX-0030-INRT, a French
573 State fund managed by the ANR under the frame programme Investissements d’Avenir
574 labelled ANR-10-IDEX-0002-02.

575 **Author contributions**

576 N.V., M.M., and N.B.G. designed the study, analyzed the data and wrote the paper.
577 N.V., M.M., D.C., B.F., M.K., V.A. and M.T. performed the experiments, analyzed the
578 data, and discussed the results. M.T. additionally commented on the manuscript.

579 **Additional information**

580 **Supplementary Information** accompanies his paper.

581 **Competing financial interests:** The authors declare no competing financial interests.

582 **Word count:** 3136

583 **Figure Legends**

584 **Fig. 1. Expression of RARs in the female gonad and germ cells during embryonic**
585 **development.** (A and B) Immunohistochemical detection of RARA and RARG (red
586 signals) on frontal histological sections of a E11.5 wild-type female embryo: expression
587 of RARG is confined to the precartilaginous anlage of a vertebra, while that of RARA
588 is more widespread and includes notably the undifferentiated gonad. (B') Same section
589 as (B) stained with hematoxylin and eosin. (C-E) Enlargement of the box in (A): RARA
590 (in red) is detected in the nuclei of some somatic cells of the gonad (arrowheads) and
591 of the coelomic epithelium; in contrast, the large, rounded nuclei characteristic of germ
592 cells (arrows) do not exhibit anti-RARA immunostaining. Nuclei are counterstained with
593 DAPI (blue signal). Ao; aorta; CE, coelomic epithelium; Go, gonad; Me, mesonephros;
594 SC, spinal cord; V, vertebra; Scale bar (in E): 160 μm (A,B,B') and 30 μm (C-E). (F,G)
595 RT-qPCR analysis comparing the expression levels and distributions of the germ cell
596 markers *Dazl*, *Ddx4* and *Kit* (F) and *Rara*, *Rarb* and *Rarg* (G) mRNAs in single germ
597 cells from control and mutant ovaries at E13.5 and E14.5. The Violin plot width and
598 length represent respectively the number of cells and the range of expression (Log2Ex).
599 The box-and-whisker plots illustrate medians, ranges and variabilities of the collected
600 data. The histograms show the percentages of expressing cells in each group. At
601 respectively E13.5 and E14.5, *Rara* is present in 96% and 83% of germ cells; *Rarb* in
602 none of germ cells since the fetus are on a *Rarb*-null genetic background (see
603 Methods); *Rarg* is present in 84% and 65% of germ cells. Importantly, *Rara*, *Rarb* and
604 *Rarg* are undetectable in germ cells isolated from the *Rar*-mutant ovaries (see main
605 text for details).

606 **Fig. 2. Markers of meiotic prophase I are robustly expressed at E14.5 in ovaries**
607 **of mutants lacking RARs.** (A) Detection of meiotic cells expressing SYCP3 (green
608 nuclear signal), REC8 or STRA8 (red nuclear signals) on consecutive, 5 μm thick,
609 transverse histological sections at four different levels of the ovaries from control and
610 mutant fetuses, as indicated. DDX4 (red cytoplasmic signal) is present in all germ cells.
611 The positions of histological sections along the anteroposterior axis is indicated in
612 terms of distance from the anterior pole of the ovary (i.e., 50, 200, 350 and 500
613 microns). + 5 μm and + 10 μm : the indicated histological sections “REC8” and “STRA8”
614 on each line are, respectively, 5 and 10 microns apart from the indicated section “DDX4
615 + SYCP3” that was used to establish the total number of germ cells. Nuclei are
616 counterstained with DAPI (blue signal). Scale bar: 60 μm . (B) Average of the total
617 number of germ cells present at the 4 different levels of the ovary illustrated in panel A
618 in 4 control (white bars) and 4 mutant (grey bars) fetuses at E14.5. (C) Mean
619 percentages of germ cells expressing SYCP3, REC8 and STRA8 in 4 control (white
620 bars) and 4 mutant (grey bars) fetuses at E14.5. The asterisk (in C) indicates a
621 significant difference ($p < 0.05$).

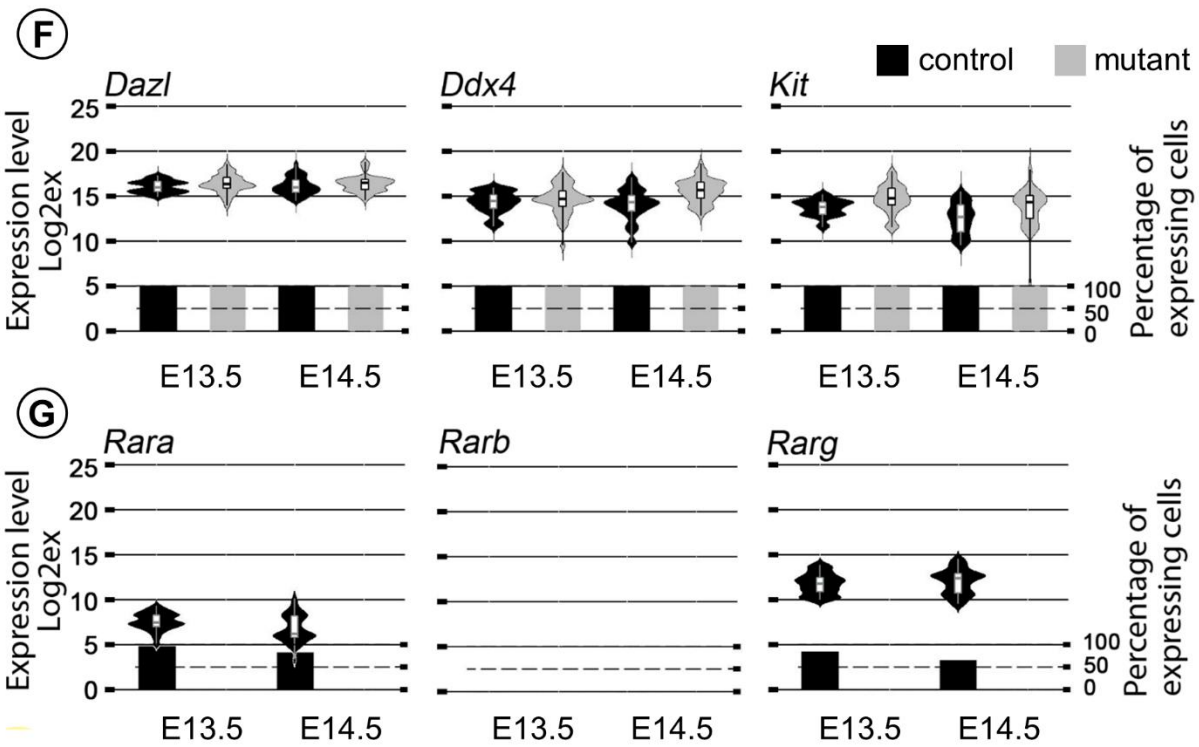
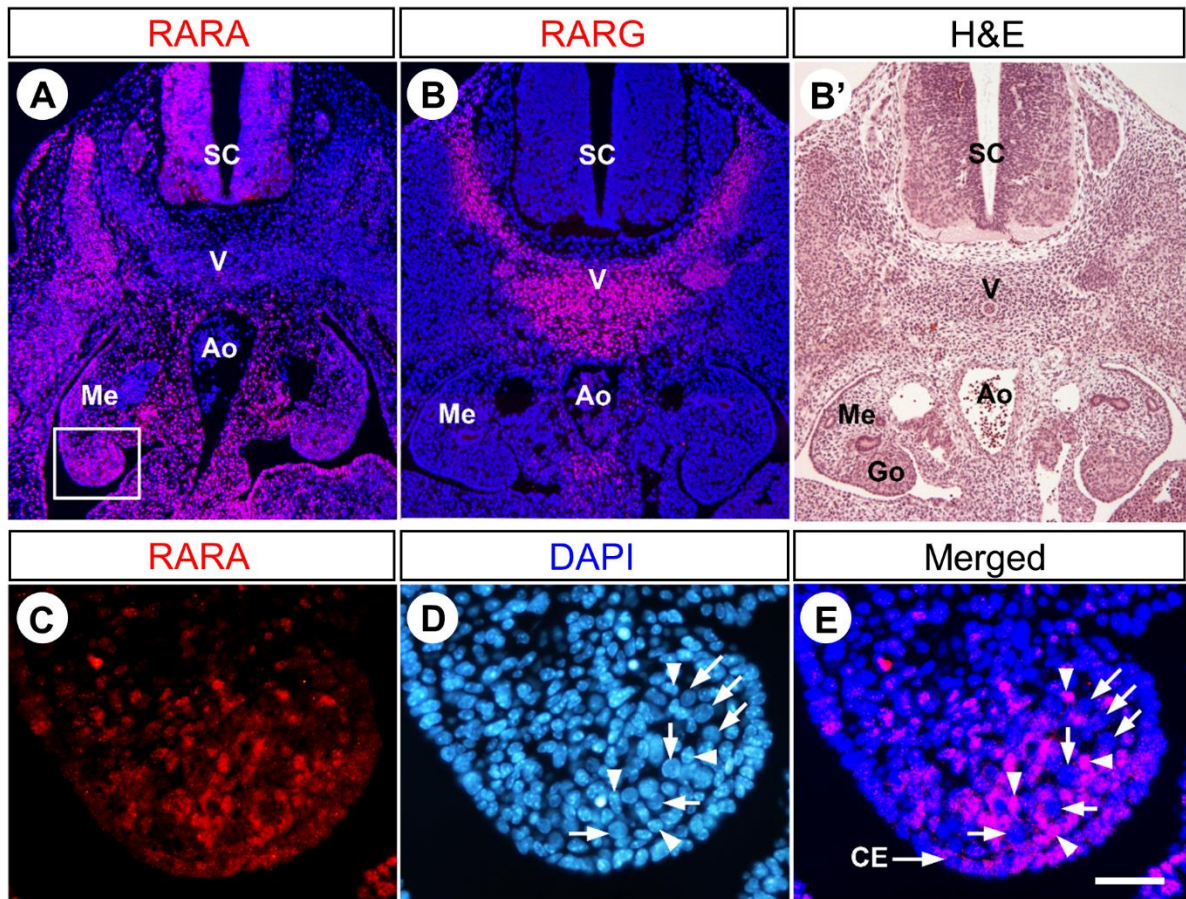
622 **Fig. 3. Evidence that gene excision has actually occurred in meiotic cells 4 days**
623 **after administration of TAM.** (A-F) Detection of the meiotic markers SYCP3, REC8
624 or STRA8 (red nuclear signals) and of mGFP (green membranous signal) on
625 consecutive, 5 μm thick, transverse histological sections at two different levels of the
626 ovary of a mutant fetus at E14.5. Efficient excision of the reporter transgene by
627 cre/ERT² is assessed by mGFP expression in virtually all meiotic germ cells. Possible
628 exceptions (i.e, red nuclei without a green contour) are indicated by white arrowheads.
629 The position of histological sections along the anteroposterior axis is indicated on the
630 left side in terms of distance from the anterior pole of the ovary (i.e., 200 and 350

631 microns). + 5 μ m and + 10 μ m: the indicated histological sections “REC8 + mGFP” and
632 “STRA8 + mGFP” on each line are, respectively, 5 and 10 microns apart from the
633 indicated section “SYCP3 + mGFP”. Nuclei are counterstained with DAPI (blue signal).
634 Scale bar (F): 60 μ m. (G,H) PCR analysis of genomic DNA extracted from ovaries of
635 control and mutant fetuses at E13.5, as indicated. (G) DNA was genotyped using
636 primers 5'-CAGGGAGGATGCTGTTTGTGTA-3', 5'- AACTGCTGCTCTGGGTCTC G-3'
637 and 5'-TACTACTAACCCTTGACC-3' to amplify the *Rara* wild-type (+, 371 bp-long),
638 the *Rara* L2 allele (427 bp-long), and the *Rara* L- (357 bp long) alleles. (H) DNA was
639 genotyped using primers 5'-TGCTTAGCATACTTGAGAAC-3', 5'-ACCGCACGAC
640 ACGATAGGAC-3' and 5'-GTAGATGCTGGGAATGGAAC-3' to amplify the *Rarg* wild-
641 type (+, 707 bp-long), the *Rarg* L2 (768 bp-long) and the *Rarg* L- (495 bp-long) alleles.
642 (I) RT-qPCR analysis comparing the levels and distributions of *Sycp3*, *Rec8* and *Stra8*
643 mRNAs in single germ cells from control and mutant ovaries at E13.5 and E14.5. The
644 Violin plot width and length represent respectively the number of cells and the range
645 of expression (Log2Ex). The box-and-whisker plots illustrate medians, ranges and
646 variabilities of the collected data. The histograms show the percentages of expressing
647 cells in each group. *Sycp3*, *Rec8* and *Stra8* are present in 94%, 91% and 72% of
648 mutant germ cells at E14.5.

649 **Fig. 4. Mutant fetuses generated upon TAM injection at E9.5 display a spectrum**
650 **of congenital defects typically observed at E14.5 in compound RAR-knockout**
651 **mutants.** Frontal histological sections at similar levels of E14.5 control (A,C,E,G,I,K)
652 and mutant (B,D,F,H,J,L) female fetuses. (A,B) In mutants, the ventral portion of the
653 retina (vR) is reduced in size in comparison to the dorsal retina (dR), the lens (L) is
654 rotated ventrally and the eyelid folds (Ey) are fused together. (C,D) Mutants display
655 mesenchymal condensations indicating the position of the salivary glands (asterisks in

656 D), but their epithelial portion (SG in C) is absent. (E,F) In mutants, the thickness of
657 the compact layer of the myocardium (green arrowheads) is markedly reduced in both
658 right and left ventricles (rV and lV, respectively). (G,H) Mutants display hypoplasia of
659 the right and left lungs (rL and lL, respectively). (I,J) Mutants, have hypoplastic kidneys
660 (K). (K,L) Mutants lack the Müllerian duct (MD in K). Sections were stained with
661 hematoxylin and eosin. H, heart; Me, mesonephros; Oe, oesophagus; Ov, ovary; PP,
662 palatal process; SC, spinal cord; SG, salivary glands; T, tongue; V, vertebra; WD,
663 Wolffian duct. Scale bar (in L): 160 μm (A,B), 320 μm (C,D,E,F,I,J), 640 μm (G,H) and
664 60 μm (K,L).

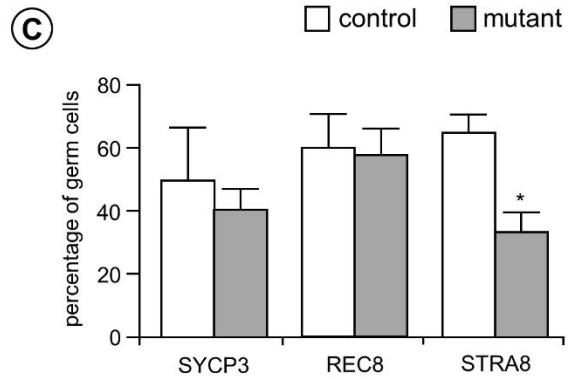
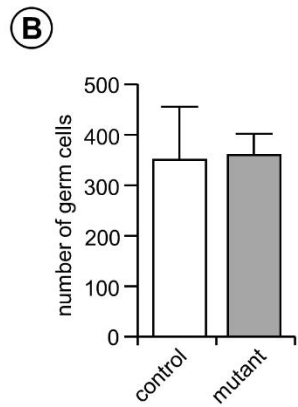
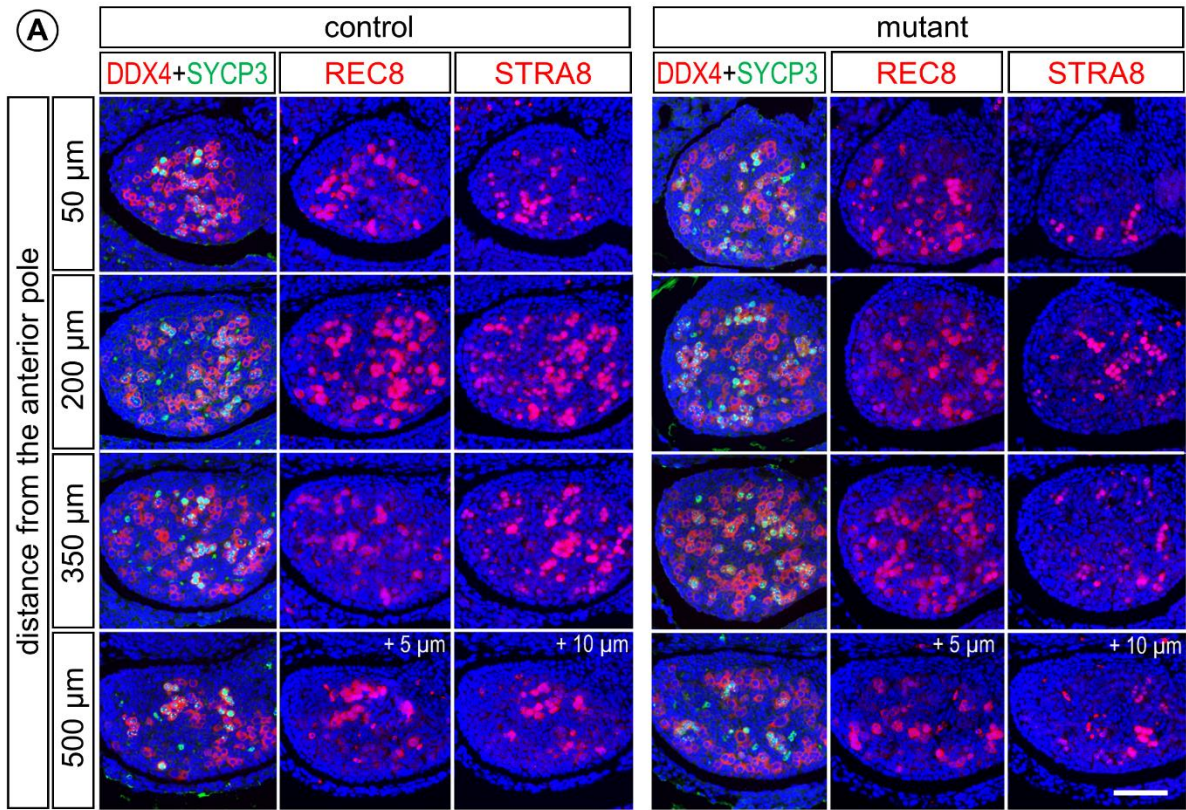
665 **Fig. 5. All germ cells have entered meiosis at E15.5 in ovaries of mutants lacking**
666 **RARs.** (A,B) Detection of germ cells (DDX4-positive, red cytoplasmic signal)
667 expressing SYCP3 (green nuclear signal): in both control (A) and mutant (B) ovaries,
668 almost all germ cells express SYCP3 at high levels; exceptions (i.e, cells expressing
669 SYCP3 at low to undetectable levels) are indicated by white arrowheads. (C,D) High
670 power magnification views of germ cells immunostained for detection of SYCP1 (red
671 signal) and SYCP3 (green signal): thread-like structures of only SYCP3 are
672 characteristic of late leptotene stages (LL), while those containing also SYCP1 indicate
673 zygotene stages (Z). (E-H) Detection of REC8 (red nuclear signal) or STRA8 (red
674 nuclear signal): both control (E,G) and mutant (F,H) ovaries contain similar small
675 numbers of germ cells expressing REC8 or STRA8. Note that (A,E,G) and (B,F,H) are
676 adjacent longitudinal sections through the same control and mutant ovary, respectively.
677 Nuclei are counterstained with DAPI (blue signal). Scale bar (in H): 60 μm (A,B,E-H)
678 and 15 μm (C,D).



679

680

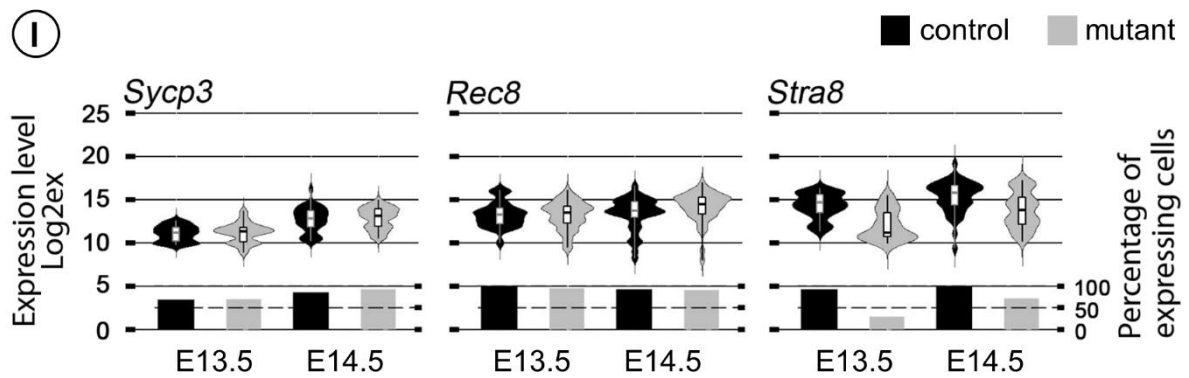
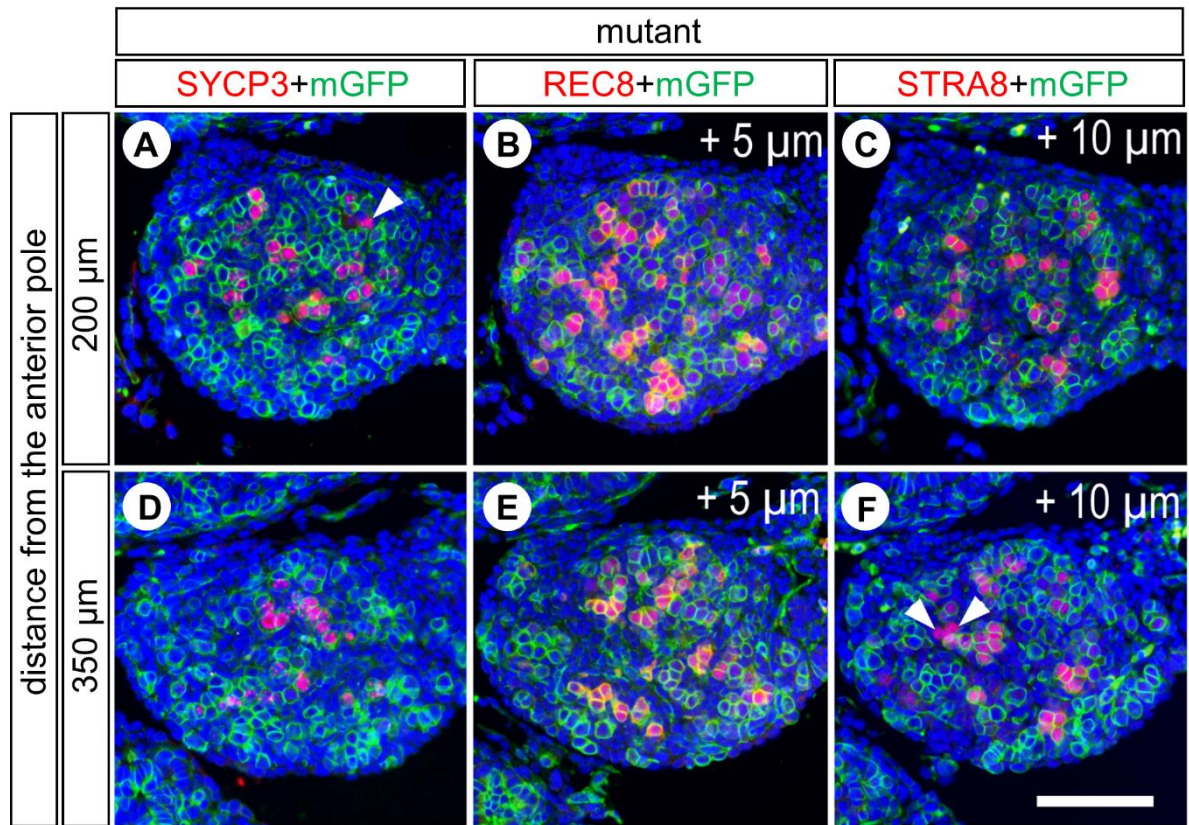
Figure 1



681

682

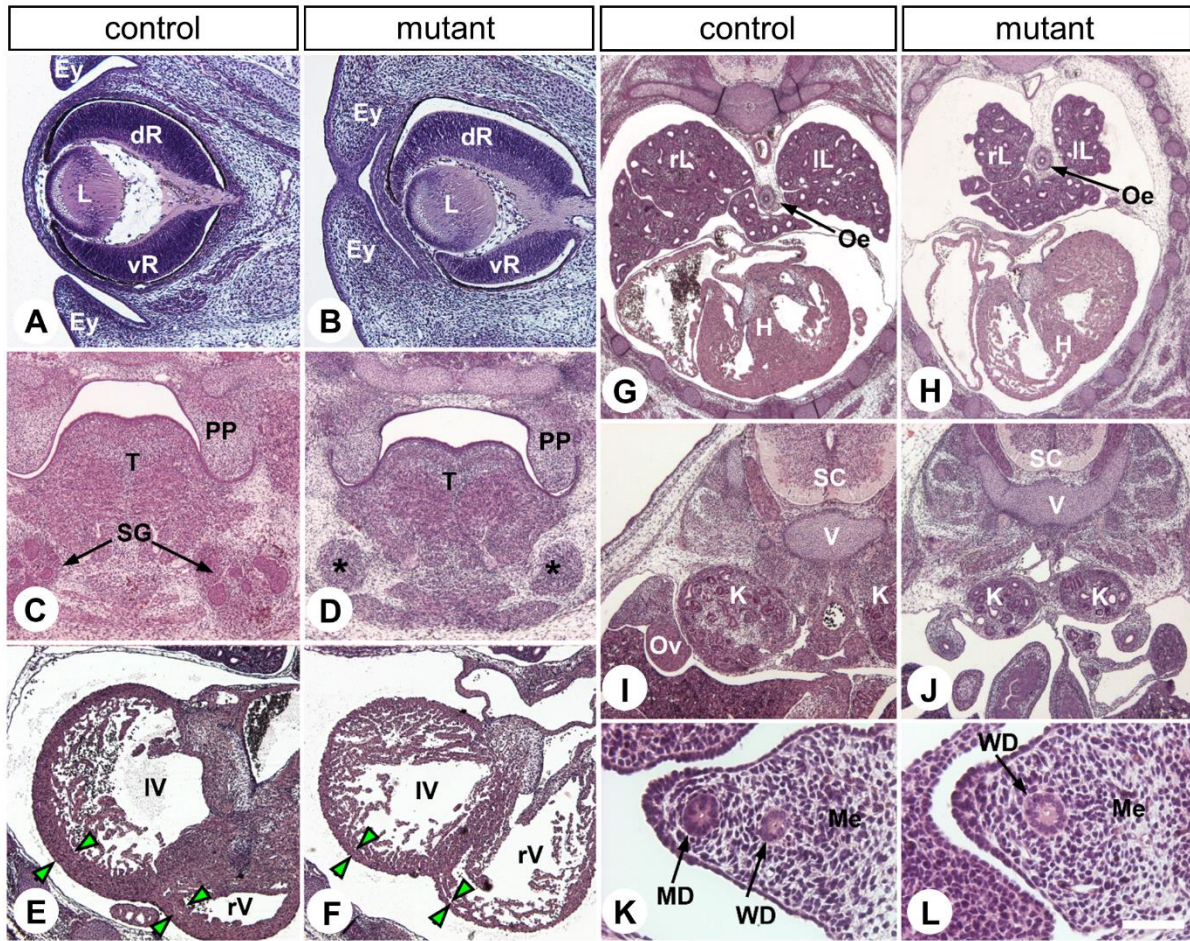
Figure 2



683

684

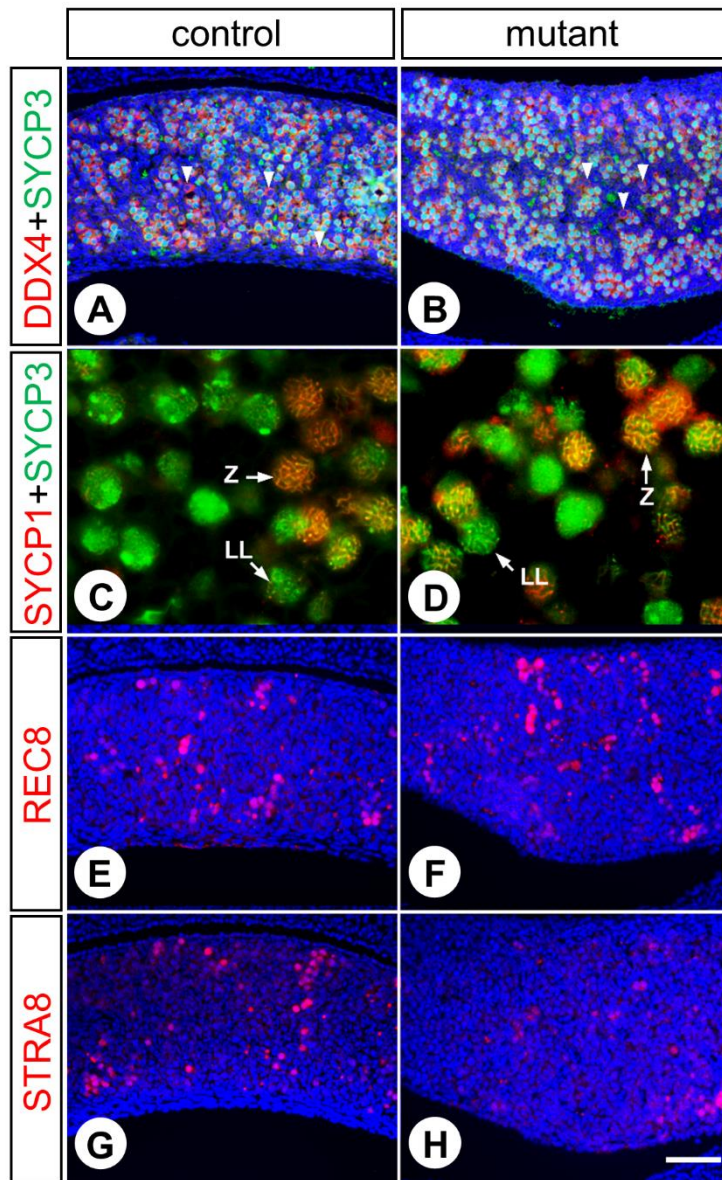
Figure 3



685

686

Figure 4



687

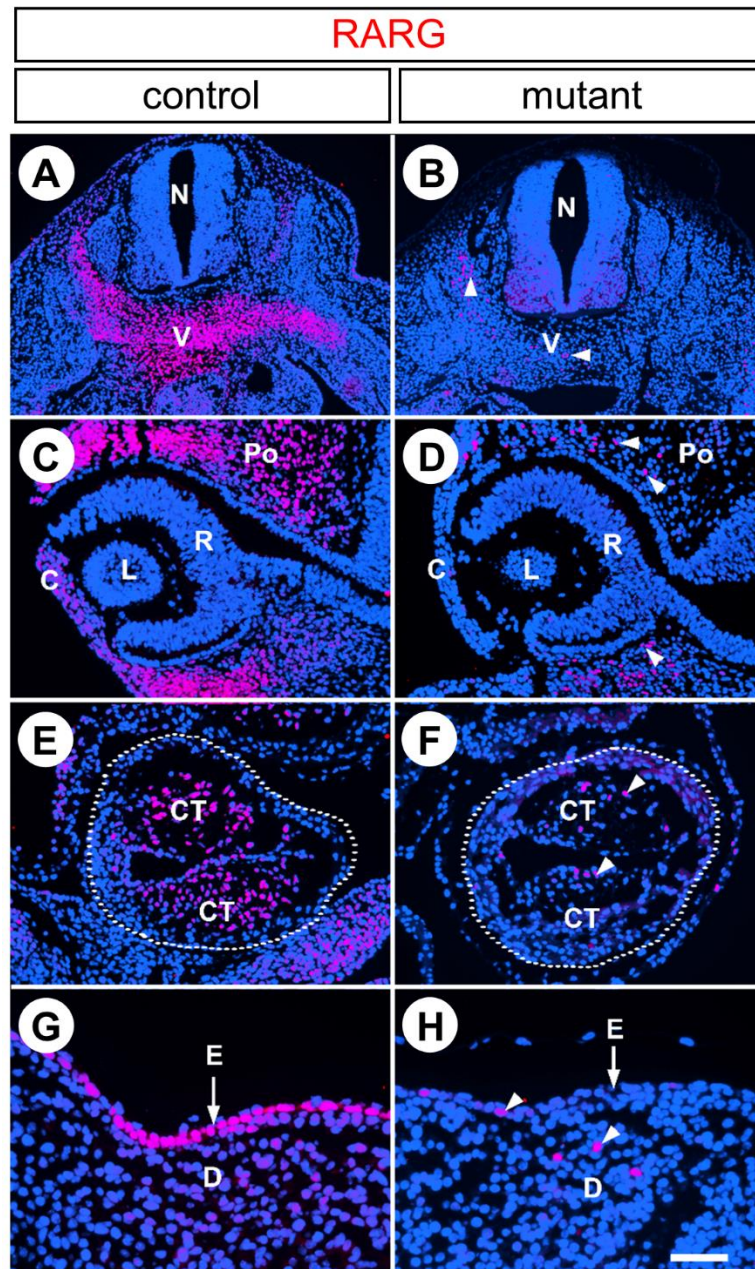
688

Figure 5

689 **MEIOSIS INITIATES IN THE FETAL OVARY OF MICE LACKING ALL RETINOIC**
690 **ACID RECEPTOR ISOTYPES**

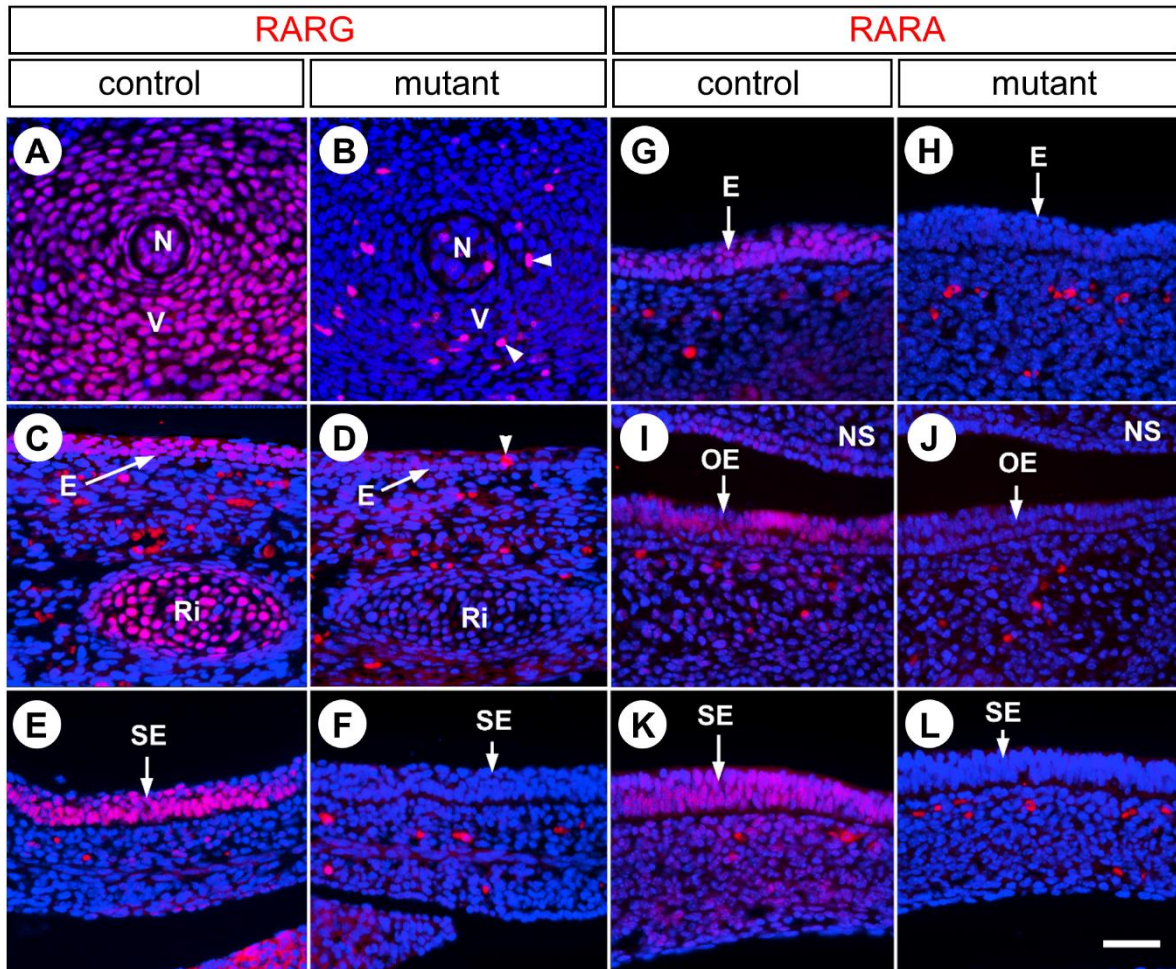
691 Nadège VERNET¹, Manuel MARK^{1,2}, Betty FÉRET¹, Muriel KLOPFENSTEIN¹, Diana
692 CONDREA¹, Violaine ALUNNI³, Marius TELETIN^{1,2}, and Norbert B. GHYSELINCK¹

693 **Supplementary Information**



694

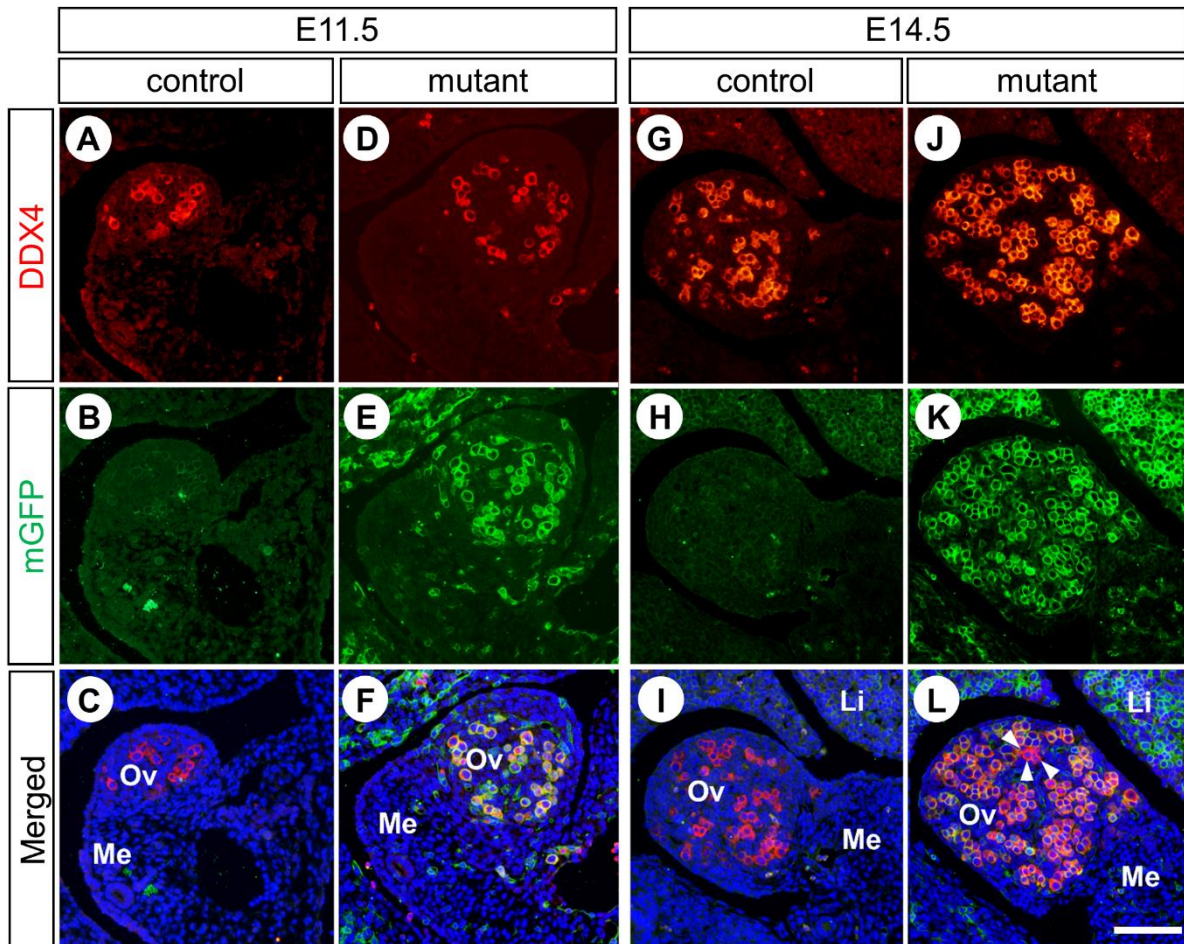
695 **Suppl. Fig. 1. Excision of RARG after administration of TAM at E10.5.**
696 immunohistochemical detection of RARG (red signal) on frontal histological sections
697 at similar levels of control and mutant embryos at E11.5, namely 24 hours after TAM
698 administration. (A,C,E,G) RARG is strongly expressed in precartilaginous vertebrae,
699 in periocular and corneal mesenchyme, in conotruncal ridges and in epidermis of the
700 control embryo. (B,D,F,H) Expression of RARG is nearly abolished in the tissues of the
701 mutant embryo. Nuclei are counterstained with DAPI (blue signal). C, cornea; CT,
702 conotruncal ridges; D, dermis; E, epidermis; L, lens; Po, periocular mesenchyme; R,
703 retina; V vertebra; The dotted lines mark off the periphery of the heart outflow tract.
704 White arrowheads indicate nuclei that are still expressing RARG in the mutant tissues.
705 Scale bar (in H): 160 μ m (A,B), 80 μ m (C-F) and 40 μ m (G-H).



706

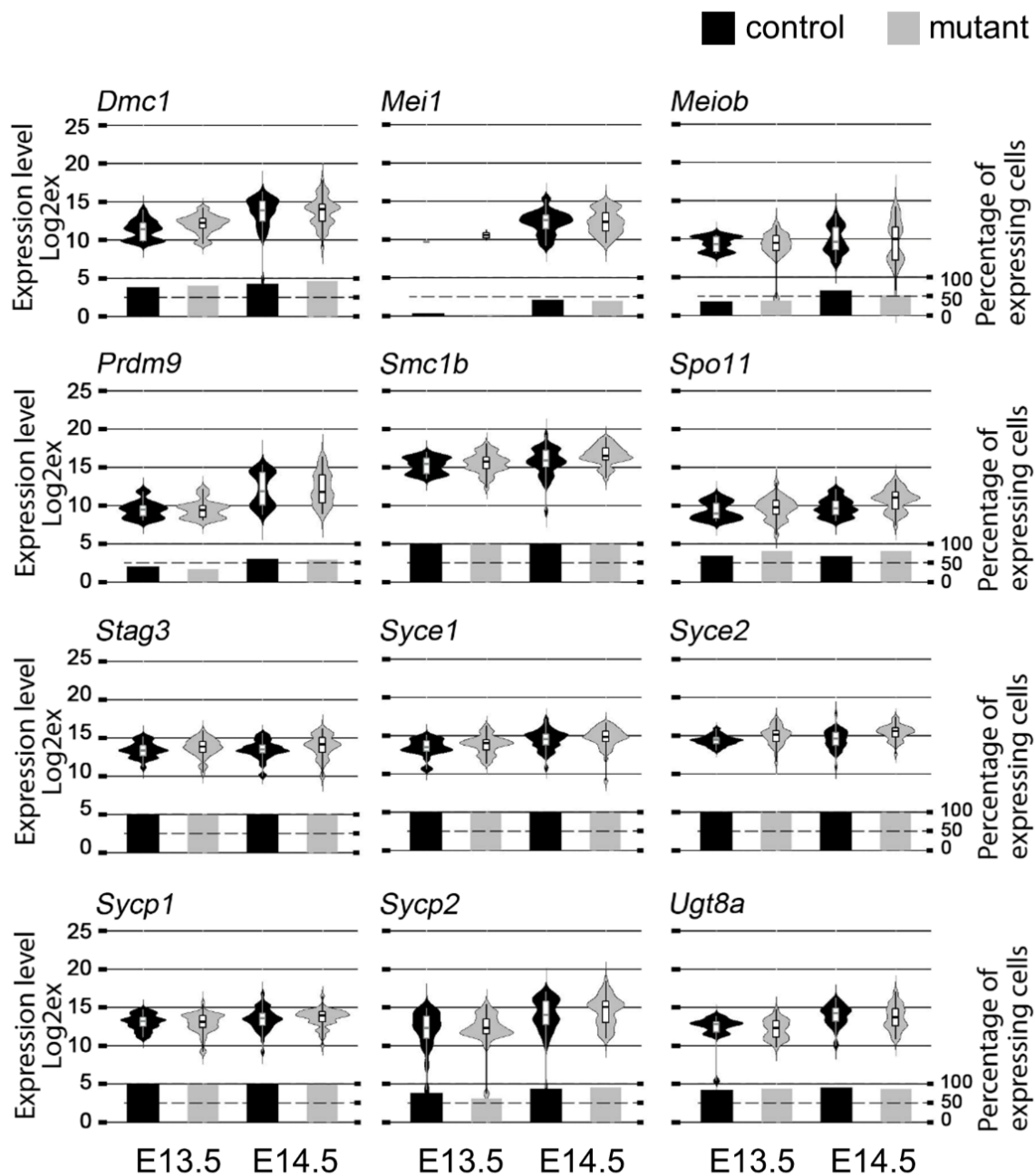
707 **Suppl. Fig. 2. Excision of RARG and RARA after administration of TAM at E10.5.**

708 Immunohistochemical detection of RARG (red signal in A-F) and RARA (red signal in
709 G-L) on histological sections of control and mutant fetuses at E14.5, namely 4 days
710 after TAM administration. (A,C,E) RARG is strongly expressed in all cartilages
711 including vertebrae (V) and ribs (Ri), as well as in the epidermis (E) and epithelium of
712 the stomach (SE) of control fetuses. (B,D,F) Expression of RARG is abolished in
713 almost all cells in tissues of mutant fetuses. (G,I,K) RARA is strongly expressed in the
714 snout epidermis (E), olfactory epithelium (OE) and epithelium of the stomach (SE) of
715 control fetuses. (H,J,L) Expression of RARA is lost in tissues of the mutant fetuses.
716 Nuclei are counterstained with DAPI (blue signal). N, notochord; NS, nasal septum.
717 White arrowheads indicate nuclei that are still expressing RARG in mutant tissues.
718 Scale bar (in L): 40 μ m (A-L).



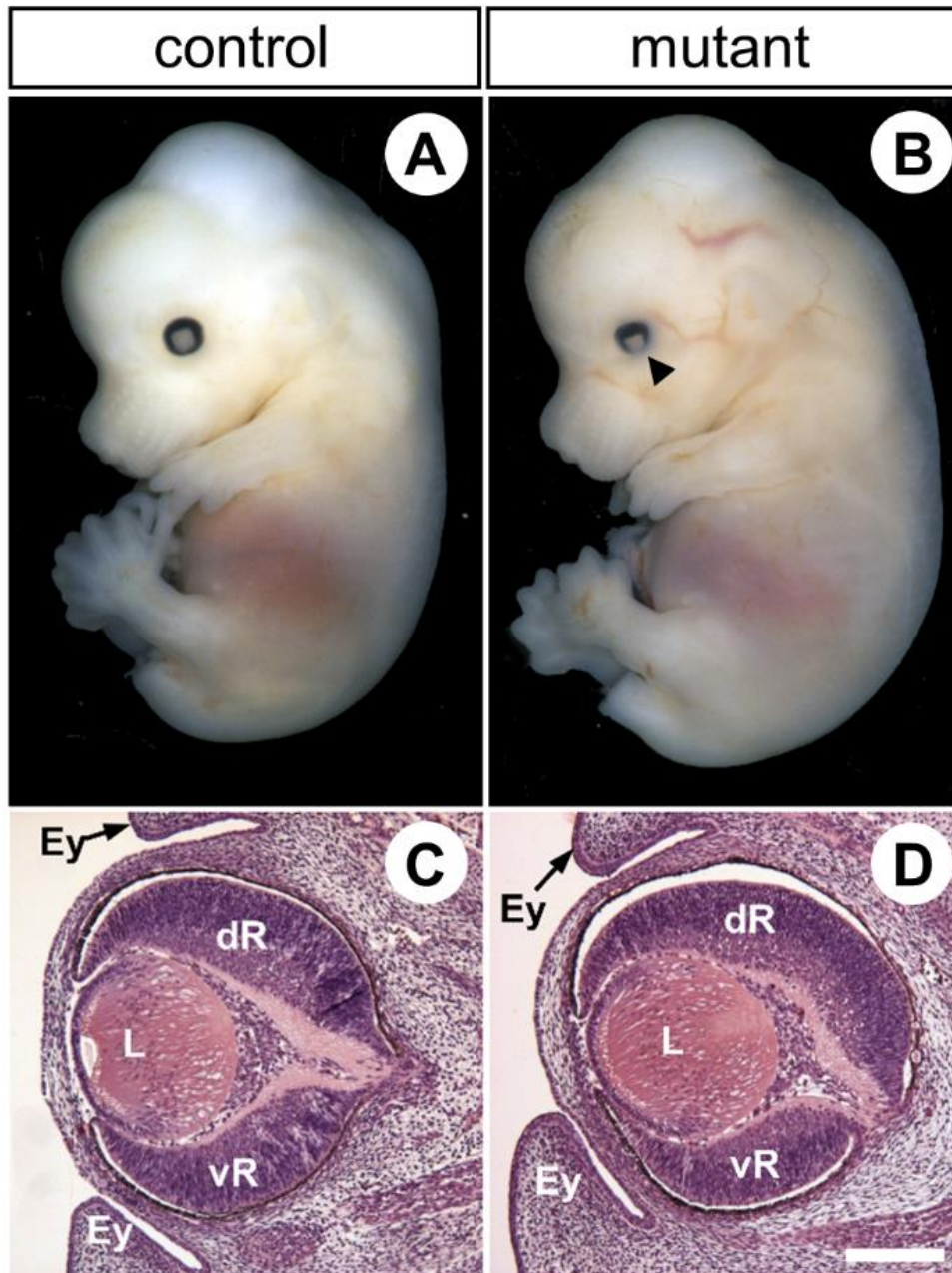
719

720 **Suppl. Fig. 3. Excision of the *mT/mG* reporter in fetal ovaries after administration**
721 **of TAM at E10.5.** Detection of DDX4 (red cytoplasmic signal) and mGFP (green
722 membranous signal) on histological sections of control and mutant ovaries at E11.5
723 (A-F) and E14.5 (G-L), namely 24 hours and 4 days after TAM administration,
724 respectively. Efficient *mT/mG* excision is assessed by GFP expression in almost all
725 germ cells (D-F and J-L); exceptions (i.e. red cytoplasm without a green contour) are
726 indicated by white arrowheads. Most importantly, GFP is never detected in control
727 ovaries, i.e., in the absence of *cre/ERT²* (A-C and G-I). Nuclei are counterstained with
728 DAPI (blue signal). Li, Liver; Me, mesonephros; Ov, ovary. Scale bar (in L): 80 μ m (A-
729 L).



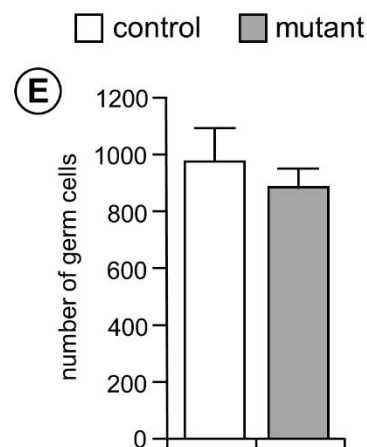
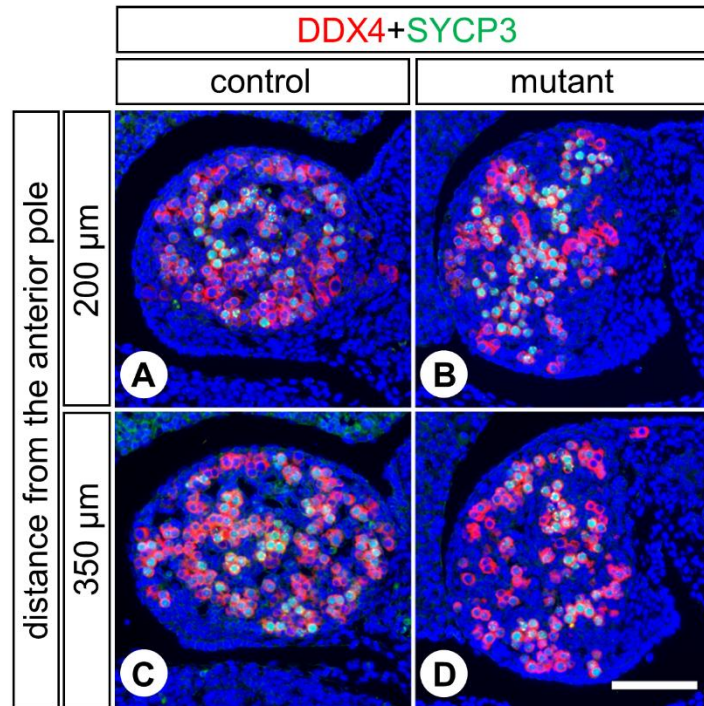
730

731 **Suppl. Fig. 4. Meiotic genes are expressed at E13.5 and E14.5 in ovaries of**
 732 **mutant lacking RARs.** RT-qPCR analysis comparing the levels and distributions of
 733 the meiotic markers *Dmc1*, *Mei1*, *Meiob*, *Prdm9*, *Smc1b*, *Spo11*, *Stag3*, *Syce1*, *Syce2*,
 734 *Sycp1*, *Sycp2* and *Ugt8a* mRNAs in single germ cells from control and mutant ovaries
 735 at E13.5 and E14.5. The Violin plot width and length represent respectively the number
 736 of cells and the range of expression (Log2Ex). The box-and-whisker plots illustrate
 737 medians, ranges and variabilities of the collected data. The histograms show the
 738 percentages of expressing cells in each group. A total of 155 cells were used for
 739 analysis (for see details, see Material and Methods).



752

753 **Suppl. Fig. 7. Congenital malformations in E14.5 mutant fetuses generated upon**
754 **TAM injection at E10.5 are restricted to eye defects typically observed in RAR-**
755 **knockout mutants.** (A,B) The pigmented retina is externally less visible in the mutant
756 (arrowhead in B). This is because the insertions of the upper and lower eyelid folds
757 (Ey) are abnormally close to each other. (C,D) In the mutant, in addition to the closer
758 eyelid folds, the ventral portion of the retina (vR) is reduced in size in comparison to
759 the dorsal retina (dR) and the lens (L) is rotated ventrally. Histological sections were
760 stained with hematoxylin and eosin. Scale bar (in D): 160 μ m (C,D).



761 **Suppl. Fig. 8. Ovaries of mutants generated upon TAM injection at E9.5 display**
762 **a normal number of germ cells and contain meiotic cells.** (A-D) Detection of DDX4
763 (red cytoplasmic signal) and SYCP3 (green nuclear signal), on transverse histological
764 sections at two different levels of the ovaries from control and mutant fetuses at E14.5.
765 (A) and (C), and (B) and (D), are consecutive histological sections. The positions of
766 histological sections along the anteroposterior axis is indicated on the left in terms of
767 distance from the anterior pole of the ovary (i.e., 200 and 350 microns). Nuclei are
768 counterstained with DAPI (blue signal). Scale bar (in D): 60 μ m. (E) Average of the
769 total number of germ cells present at the 7 different levels of the ovaries, 75 microns
770 apart, in 3 control (white bar) and 3 mutant fetuses (grey bar).

Antigen	Species	Reference	Source	Secondary antibody
DDX4	Rabbit	ab13840	Abcam	Cy3-conjugated donkey anti-rabbit IgG
mGFP	Chicken	GFP-1020	Aves	Alexa Fluor 488-conjugated goat anti-chicken IgG
RARA	Rabbit	RPalph(F)	Gaub et al., 1992*	Cy3-conjugated donkey anti-rabbit IgG
RARG	Rabbit	8965S	Cell signaling	Cy3-conjugated donkey anti-rabbit IgG
REC8	Rabbit	HPA031729	Sigma	Cy3-conjugated donkey anti-rabbit IgG
STRA8	Rabbit	ab49602	Abcam	Cy3-conjugated donkey anti-rabbit IgG
SYCP1	Rabbit	ab15090	Abcam	Cy3-conjugated donkey anti-rabbit IgG
SYCP3	Mouse	ab97672	Abcam	Alexa Fluor 488-conjugated donkey anti-mouse IgG

771 **Suppl. Table 1. Antibodies used in immunohistochemistry experiments.** *Gaub
772 *et al.*, (1992) *Exp. Cell Res.* 201:335-346.

Gene	Forward primer sequence (5' to 3')	Reverse primer sequence (5' to 3')	Amplicon size (bp)
<i>Actb</i>	CTAAGGCCAACCGTGAAAAGAT	CACAGCCTGGATGGCTACGT	195
<i>Dazl</i>	GTCCTTACATGTACCATTCTGTGAC	GACTCCAACAAAACAGCAGACAA	143
<i>Ddx4</i>	GTTGAAGTATCTGGACATGATGCAC	CGAGTTGGTGCTACAATAATACT	299
<i>Dmc1</i>	GCGGCTACTCAGGTGGAAAG	TGGTCTACGTTGAAGCGGTC	97
<i>Kit</i>	CACTCACGGGCGGATCACAAA	CCACTTCACGGGCAGTCGTGC	106
<i>Mei1</i>	ACGCATCCAAAGCTGATGGAGGTT	CTTCAGCTCCAGGGTCAGTCGTAT	132
<i>Meiob</i>	GAAGTGCATGGCAGCAACTG	GCTGTTCCACTGTATAGACATCA	188
<i>Prdm9</i>	TGGCTGATTACCAAGGGAAGAAAC	TCCCCATACCAGACCAGAAGCTCA	200
<i>Rara</i>	AAATCATCCGGCTACCACT	TCTGGATGCTTCGTGGAA	73
<i>Rarb</i>	GTGTTACCTTTGCCAACCAG	TTTAGTGCTTCCAGCAGTGGT	155
<i>Rarg</i>	TCTTCTGGCTACCACTATGGGGTCA	GCAGTACTGGCATCGATTTCTGG	147
<i>Rec8</i>	ATTCGACACCTTTTAGAGGCTG	AAGTCTCCTCGACTGATCTCTG	203
<i>Smc1b</i>	GCATGGATTGCTTGGAAAGATA	CTGACGTTTTCCCTCATGGTT	158
<i>Spo11</i>	TTGATCCCACTGACAAAGCATGAC	GTCTGACGACAGCAAGGTCAAG	156
<i>Stag3</i>	GCTTGGAAAAGCACTTGGAG	GCTTCTGGCAAAGTCCACTC	155
<i>Stra8</i>	ACAACCTAAGGAAGGCAGTTTAC	GACCTCCTCTAAGCTGTTGGG	173
<i>Syce1</i>	GGAAAAGCATGGGGTACAGATCC	GCTGTCTCCTCGTGGACTTCTAC	105
<i>Syce2</i>	CAAGTCTGCCAAACTGTGGAAC	GCAGAAGTCAGCATTACCATCT	106
<i>Sycp1</i>	AGGACCGTTGGACAACGATTGC	CCTTGGTAAAGTTTGGCTCTCTTGG	160
<i>Sycp2</i>	GACTGAAACCGAATGTGGA	TGTGGGTCTTGGTTGTCCTTT	165
<i>Sycp3</i>	GGGGCCGGACTGTATTTACT	AGGCTGATCAACCAAAGGTG	169
<i>Tbp</i>	TGCTGTTGGTGATTGTTGGT	AACTGGCTTGTGTGGGAAAG	99
<i>Ugt8a</i>	CTGCAGAGGTGGGTAAGTGG	GCAGGTCATTTTGAGGCAGCC	214

773 **Suppl. Table 2. Primers used for RT-qPCR on single cells.**